MICROSTRUCTURE BIO-MATERIAL FOR BEHAVIORAL ANALYSIS

A Dissertation

by

PUNSIRI LAKRUWAN SAMARASINGHE

Submitted to the Office of Graduate and Professional Studies of
Texas A&M University
in partial fulfillment of the requirements for the degree of

DOCTOR OF PHILOSOPHY

Chair of Committee,	Jun Kameoka
Committee Members,	Chin Su
	Chanan Singh
	Kung-Hui Chu
Head of Department,	Chanan Singh

December 2014

Major Subject: Electrical Engineering

ABSTRACT

Biological applications have a limitation of creating tissue like structures in order to mimic the advanced real like structures, such as human tissues in a small scale. Conventional methods of using lab mice for cancer behavior have limitations due to observation complications. Fabricating an artificial human tissue which can behave similar to a human body tissue consists of components, such as Laminin and Collagen. Collagen in human tissue has elements, such as integrin and serum. Creating serum based proteins are somewhat challenging due to the conditional requirements. This particular approach will address the primary state of the art technique of observing the interaction with cells by mimicking the organs on a chip with blood circulation using a micro-fluidic pump. Bio-material hydrogel structures implanted on a silicon polymer based chip described in this thesis will overcome the limitations of in-vitro analysis.

Water purification has become a vital issue in developing countries of the world. Water pollution due to Ammonia has been one of the major concerns with industrial revolution. Purifications were mainly done by chemical methods that can cause human health concerns. The analytically demonstrated method in this thesis using bio-compatible hydrogel will address a new dimension to the water conservation method without causing health issues and eliminating the environmental pollution due to complicated degradable structures. Filtration and efficiency are among the main concerns of using bacteria types such as AOB/NOB directly without encapsulating. Application of using bio-compatible hydrogel based dual encapsulated single pallet

structure described in this thesis will address the issue of filtering capability. Pallets can be removed once nitrified, without letting it grow inside the water contaminating aqua based living breads and plants. The process will improve the efficiency of Ammonia removal due to encapsulation.

Drug delivery using micro locomotives in neuro-surgery has become one of the future concerns with the development of science. Conventional delivery systems such as vaccines and open surgeries take longer response time once surgeries become more complex. Moreover there is a risk factor of injuring healthy nerves in the organ. Drug delivery approaches of drug encapsulated microspheres and drug embedded nematodes described in this thesis become more applicable to complex scenarios. Nematodes become useful in the future of microsurgeries, as many biologists are focusing on using their healthy nerves to implant in humans. Therefore, such applications like magnetizing nematodes help move locomotives to targeted locations and capture scan images for future medical approaches.

DEDICATION

To my late father Mr. S.A.P. Samarasinghe. Thank you for helping me to continue my higher educations and courage you have given me during the short life.

ACKNOWLEDGEMENTS

I would like to thank my advisor Dr Jun Kameoka for all the guidance. I highly appreciate the support given to me by my committee members Dr Chu, Dr Su, Dr Singh for their precious advices they have provided.

My gratitude goes towards Dr Chao-Kai and Dr H. Yamaguchi of M.D.Anderson Cancer Center for their support. I would like to thank Dr Yeh (Bio-medical Engineering) for giving me the opportunity to use his open access tissue culture facility to grow our MCF 7 and MDA 231 cells.

I appreciate the help given by Dr Roula Mouneimne in veterinary school imaging center for helping me take images of dead/alive bacteria cells using their confocal microscope, lots of merits for sharing her experience with me and working with me patiently to get the best possible images. I would also like to thank Texas A&M Material Characterization Facility (MCF) and Aggiefab staff for providing me training and allowing me to use their facility for my fabrication process.

Finally my heart felt gratitude goes towards my past colleagues Dr Pei-Hsiang Tsu and Dr Sungmin Hong for sharing their valuable experiences.

NOMENCLATURE

MCF	Michigan Cancer Foundation
MDA	M D Anderson
DMEM	Dulbecco's Modified Eagle Medium
LOC	Lab On a Chip
PDMS	Polydimethylsiloxane
ECM	Extra Cellular Matrix
RPM	Revolutions Per Minute
PEG-DA	Polyethylene (glycol) Diacrylate
UV	Ultra Violet
PPO	Poly (ethylene glycol)-block-poly(propylene glycol)-block-poly(ethylene glycol)
AOB	Ammonia-Oxidizing Bacteria
NOB	Nitrite-Oxidizing Bacteria
C-Elegans	Caenorhabditis Elegans
PAH	Poly-allylamine hydrochloride
PBS	Polly Buffer Saline

TABLE OF CONTENTS

Page

LIST OF FIGURES

LIST OF TABLES

CHAPTER I

INTRODUCTION AND LITERATURE REVIEW

1.1 Development in Bio-Medical & Environment Engineering

Human being has been moving from several generations with the transition from early stage to industrial economy. Pollution and disease are among the major concerns with the industry growth. Due to the fact the bio-technology and medical engineering started to bloom up in late 90's. Health, Environment and treatments are one of the major concerns among the future generations.

Health wise, Cancer has been among the most spoken research topics in medical industry. There have been many controversial issues related to in-vivo and in-vitro analysis of tumor analysis and metastasis analysis. Past few decades most of the research has been done by using lab mice as the in-vivo analysis. Major drawback of using a living organism such as a mouse would be the real time data analysis, due to the fact that the growth can be observed by killing the living organ. Real time data analysis at any given time would be the major advantage of using LOC (Lab On a Chip) device as the metastasis testing.

Major pollution sources of Environment are due to the Toxins such as Ammonia. Many Civil Engineering researches & environmental engineers has been testing variety of methods to reduce the water pollution by ammonia using a certain types of bacteria. One of the limitations however was keeping the optimum reaction ratio for the

maximum performance inside the liquid. Microfluidic devices and types of bio compatible hydrogels have been able to address the above issues.

1.2 Fabrication Process

Lithography process has been the foundation for the micro-device fabrication. Devices were fabricated using PDMS molding technique which is very economical and produce high throughput of devices. Device bonding were done using the Oxygen plasma.

3-D device pattering is among another method which has been developed over the years; however it was more innovatively involved with some modification in this particular 3D molding. 3D molding technique has been applied in few literature journals as a single layer technique, However it's not been use as a multiple layer fabrication technique due to the fabrication and alignment difficulties. Major drawbacks of using 3D dual encapsulation of different types of components in hydrogel are, deploying a mold which can hold the liquid more effectively. Patterning 3D mold by spin-coating at desired RPM using PDMS would effectively outcome the 3D hydrogel patterning with the help of some alignment marks, as the 3D-Lift off process.

Hydrogels are among the most outspoken topics in the recent medical development due to the bio-compatibility & 3D patterning ability. Matrigel, Collagen, Mebiol Gel and PEG-DA are among the vastly used bio-compatible hydrogels. PEG-DA becomes more applicable in water based environmental dual component encapsulation due to its cross-liking ability via UV exposure and water insolubility.

1.3 Significance of Research and Analysis

As several topics has been addressed in this dissertation; there are several major advantages of this particular fabrication process and data Analysis. This could affect many ways to future research and commercial type bio-medical industrial device fabrications in large amounts. As discussed in the LOC device fabrication, it could be used to produce more samples using large amount of devices. 3D patterning mold technique can produce more samples at a time analysis it will produce a higher throughput. Since all the devices are made out of PDMS, which will reduce the cost of fabrication process. Since small amount of samples of bio-material has been used in each scenario, it will reduce the sample cost and reduce the waste of material. Since each sample can be observed and analyzed at a time, data analysis will be more accurate. Real time anti-cancer drug analysis has been among the challenging mechanisms in previous research methods due to the in-vivo analysis. By creating an in-vivo tissue like structure on a chip using matrigel as the bio-material, it will overcome the challenge of anticancer drug screening response more in to detail under the fluorescence imaging microscope.

CHAPTER II

CANCER METASTASIS ON A CHIP (CMOC)

2.1 Introduction

Cancer drugs has been used various varieties for treatments for different types of cancer. Breast cancer, colon cancer, skin melanoma, lung cancer are among main types of cancers researchers has focused on recent past. Limitation of the devices for testing drugs was the major drawback during the research in past. This section discuss about deploying fabrication techniques of micro-fluidic development for cancer metastasis behavior with drugs and how they responds to different types of breast cancer cells. Here the process mimics the human body by using micro-pump for the circulation and constructed the body temperature environment by conduction the experiment inside the incubator.

2.1.1 Introduction to Matrigel

Matrigel is a type of a bio-compatible hydrogel consists of structural proteins of Entactin, Collagen and Laminin. Matrigel is the substitute of the human tissue used in this process. [1] Collegen has an attraction to the cell matrix since collagen IV has perfect adhere to the cells. [2]

Structure of cells consists of integrins covered by an extra cellular matrix, which consists of α and β chains. There α and β subunits binds each other and crates different

types of αβ legends. Integrins carrying α1β1 and α2β1 has more binding capability with collagen receptors. [3]

2.2 Experimental

2.2.1 Fabrication of the Metastasis Device

Photolithography technique has been used for the basic fabrication process of the devices on a silicon wafer. Process was done by spin coating SU-8 on a silicon wafer. SU-8 is a negative photoresist, standard procedure of baking and UV exposure of 1.4mJ/sec UV source for 60 seconds was used to transfer the pattern. After the exposure the device has gone through the post exposure bake and resists developing cycle to fabricate the device.

Once the device has been fabricated, mold of the device had been done using PDMS (Polydimethylsiloxane) SYLGARD 184 Silicone Elastomer Kit, Dow Corning by thoroughly mixing as Curing Agent 10:1 mixture. Premixed polymer was stirred and poured on to the patterned silicon wafer and backed at 65^{o}C for solidifying as seen in Figure 1. Solid device was then treated with a glass slide via Oxygen plasma treatment with parameters of 25W power, 100miliToor Pressure, for 30 seconds with 5% Oxygen.

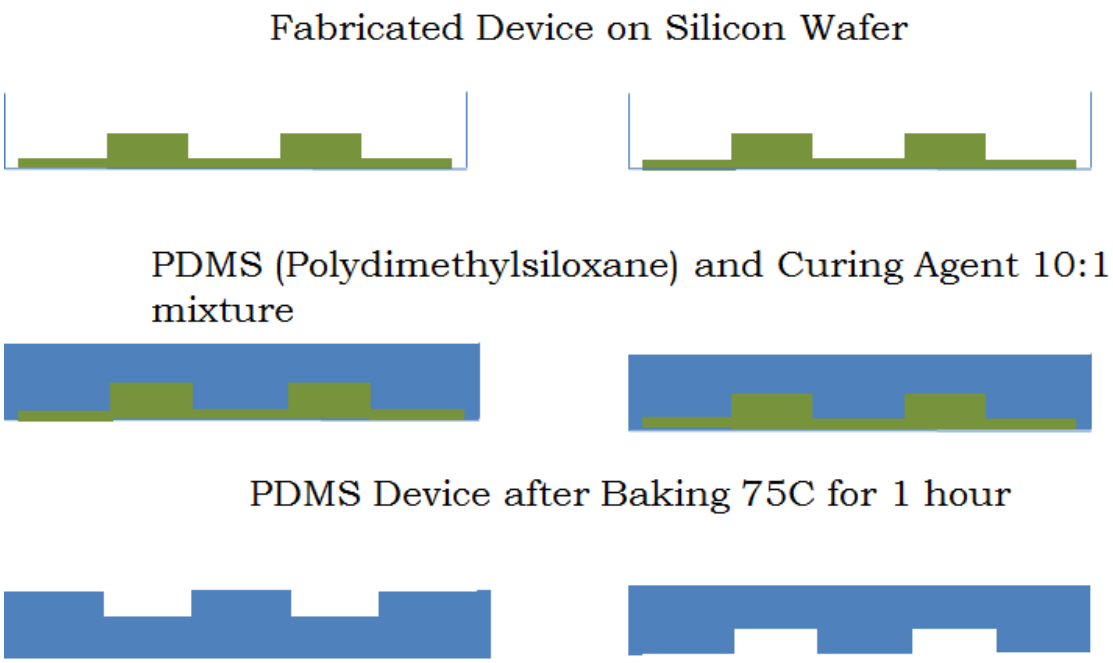

Figure 1 Fabrication process of PDMS mold

2.2.2 Application of Matrigel Coating on the Device

Matrigel mainly consists of Collagen and Laminin which are temperature sensitive material. Cross-lining of Matrigel occurs at 37^{o}C and liquidize at 4^{o}C. [4] PDMS device was placed on a cold surface such as an ice pack prior to the application of matrigel. Once injected metrigel coated device was incubated for ½ hr at 37^{o}C incubator for better cross-linking as seen in Figure 2.

Bonded metrigel has an auto-fluorescence effect as seen in Figure 3. Metrigel applicator area was distinguished by the fluorescence effect as seen in Figure 3(a).

2.2.3 Cell Culturing and Preparation

MDA 231 and MCF 7 cells were grown inside CO2 water-jacket incubator with 5% CO_2 and 37.5^{o}C. Cells were prepared immediately prior to the experiment. First DMEM (Dulbecco's Modified Eagle Medium) were extracted out by 5ml mechanical pipet and cells were washed with 2ml of PBS. Once all the contents and residues were washed out, cells were trypsinzed by 1ml of trypsin. Trypsinized cells were then transferred in to the incubator for 3 minutes for the cells to be detached from the culture flask surface. Cells were then removed by 5ml of DMEM and transferred in to a 50ml sterile tube. Transferred tube was then centrifuged at 3000rpm for 3 minutes. Cell pallets will be visible inside the bottom of the tube once centrifuged. Remaining solution was then extracted out in order to remove the trypsin, since leftover trypsin will result different form from natural human cell conditions. DMEM mixed extracted cells were then counted by the cell counter in order to get the desired cell count for the experiment of 10^6 cells/ml.

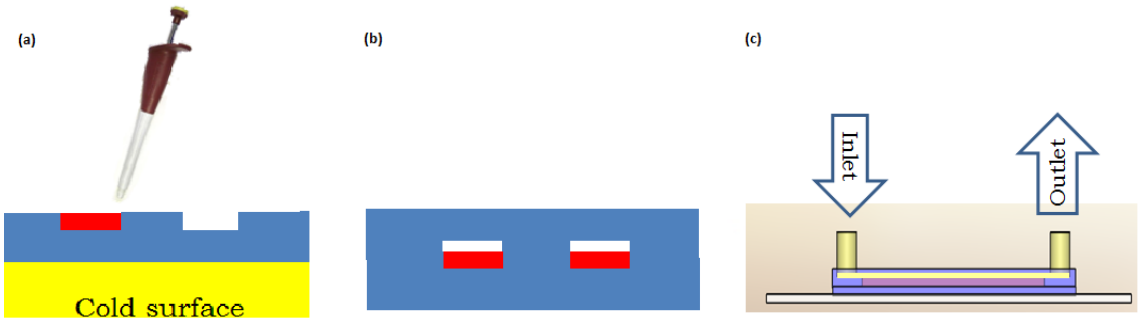

Figure 2 (a) Application of matrigel on PDMS block top of a cold surface, (b) Cross-section views of gel coated channel, (c) Complete channel for cell adhesion

2.3 Result

2.3.1 Cell Adhesion Analysis

Cell Adhesion analysis was done using the syringe pump with flow rates of 24ul/min, 16ul/min, 12ul/min, 8ul/min, 5ul/min, 3ul/min, and 2ul/min. Number of cells attached on the cell surface was analyzed for 15mins of time period for MDA 231 cells. According to the result velocity can be categorized in to two different regions: 1) Adhesion 2) Linear region as seen in Figure 4. 5ul/min and 3ul/min flow velocities demonstrated cell adhesion due to the collagen ECM interaction, while 3ul/min demonstrated higher number of cell adhesion of 20 MDA 231 GFP cells as seen in Table 1. Therefore 3ul/min flow rate applied as the optimum condition as seen in Table 2. Attachment analysis was done for the MDA 231, MDA 231 (Starvation), MCF 7, MDA 231 with paclitaxel (10nM) for the 3ul/min flow rate. Paclitaxel is a widely used anticancer drug which can cause the damaging integrin by not letting them attach to the cancer cell. **[**5] Test results prove that this particular application can mimic the human tissue inside the circulation device.

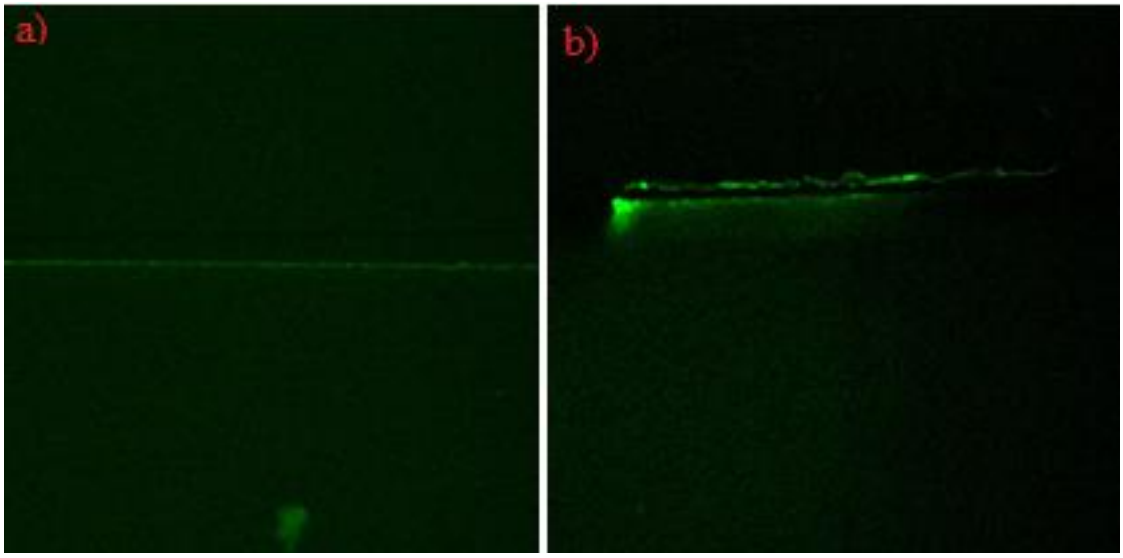

Figure 3 (a) Fluorescent image of channel, (b) Fluorescent image of cross section of the channel

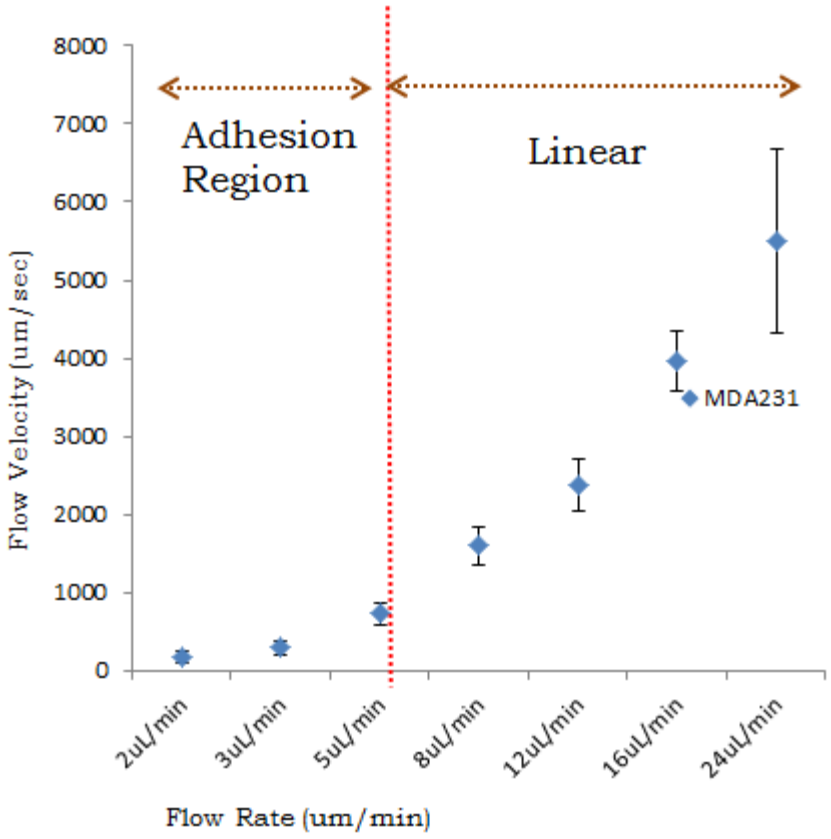

Figure 4 Number of cells for different flow velocities

Table 1 Cell adhesion for different flow velocities

Flow Rate	24ul /min	16ul /min	12ul /min	8ul /min	5ul /min	3ul /min	2ul /min
Number of Cell Adhesion	0	0	0	0	5	20	0

Table 2 Cell adhesion for 3ul/min with different cell types

Cell Type	MDA 231	MDA 231 starvation	MDA 231 (paclitaxel 10nM)	MCF 7
3ul/min	20	8	1	0

2.3.2 Cell Attachment Due to Matrigel

Flow velocity change and the cell adhesion due to Matrigel were confirmed by using polystyrene beads of 10um. Beads were injected via the syringe pump at 3ul/min flow rate mixed with paclitaxel (10nM) and compared with the flow velocity of beads as seen in Figure 5. Beads were flown in the same manner as cells and beads didn't demonstrate the attachment as the cell. This particular mechanism demonstrated the cell attachment was due to the extras cellular matrix (ECM) attachment due to the interaction between ECM to the Laminin & Collagen in matrigel.[6]

2.3.3 Flow Velocity Due to ECM Interaction Characteristics

Following experiment was done for MCF 7, MDA 231(starvation) and MDA 231. 10uM polystyrene beads have been used as the control in this particular scenario since they does not consists of an ECM structure. MCF 7 is a less malignant breast cancer cell type which doesn't metastases. MDA 231 starvation cells were prepared by removing the serum mixed culture medium and growing the cells inside culture medium without serum for 24hrs. Serum provides the proteins and nutrition for the cell growth; once the serum was removed they move on to a starved stage which is less active. MDA 231 is the highly malignant cancer cell type in this category. Above category has been tested for their flow velocity characteristics by flowing them inside the matrigel device at 3mL/min. Polystyrene beads demonstrated highest flow velocity due to their non-interaction with matrigel, while MDA 231 high malignant cells demonstrated lowest flow velocity due to their high interaction with ECM structure as seen in Figure 6.

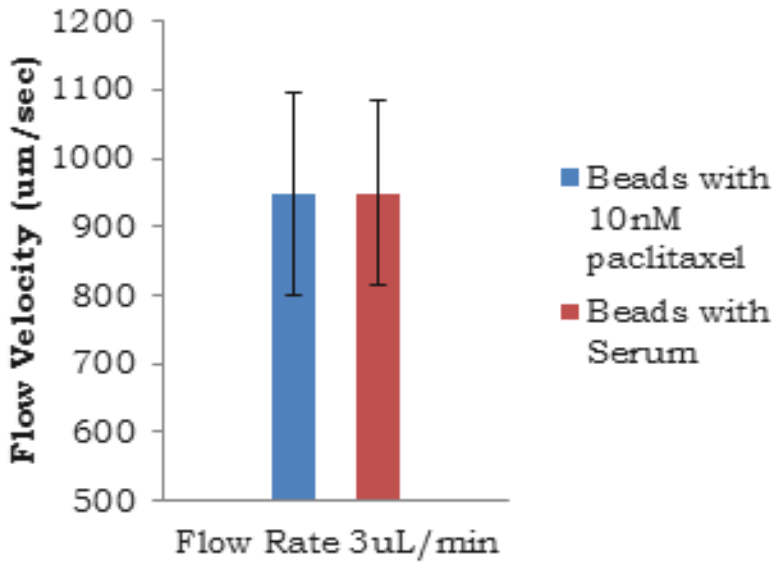

Figure 5 Flow velocity characterization with polystyrene beads

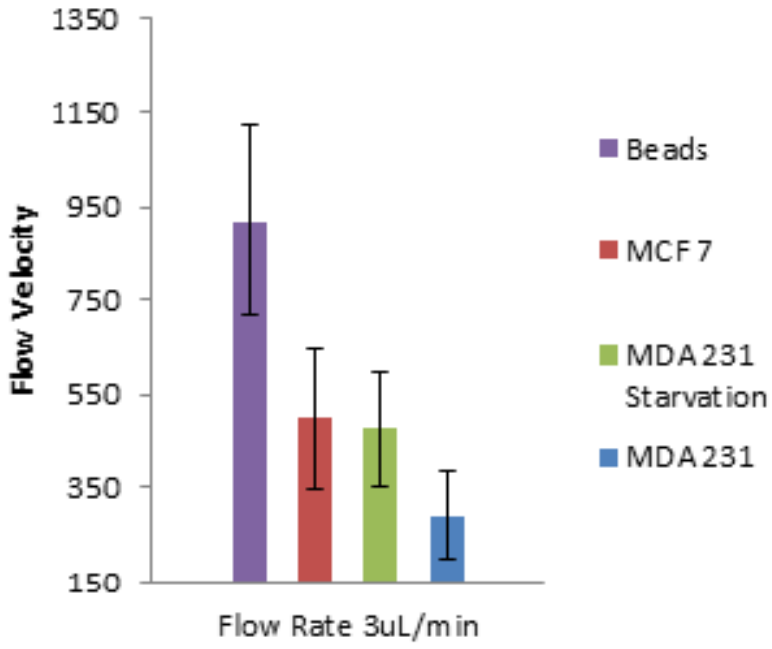

Figure 6 Flow velocity characterization with different types of cells at 3uL/min flow rate

2.3.4 Velocity and Attachment Change Due to Chemotherapy Drugs

Paclitaxel is one of the chemotherapy drugs used in cancer treatments. Following concentrations of 100nM, 10nM, 1nM, and 0.1nM of paclitaxel been applied with MDA 231 cells. Cell flow velocities were tested for 3uL/min flow rate characteristic of the flow pump. Paclitaxel chemotherapy drug works more effectively at 0.1nM for the practical applications in health care and that is the recommended concentration to use. Higher the concentration of chemotherapy drug it works inefficiently as seen in Table 3.Cell flow velocity and the numbers of cells attached were different as the paclitaxel concentration changes as seen in Figure 7 and Table 3.

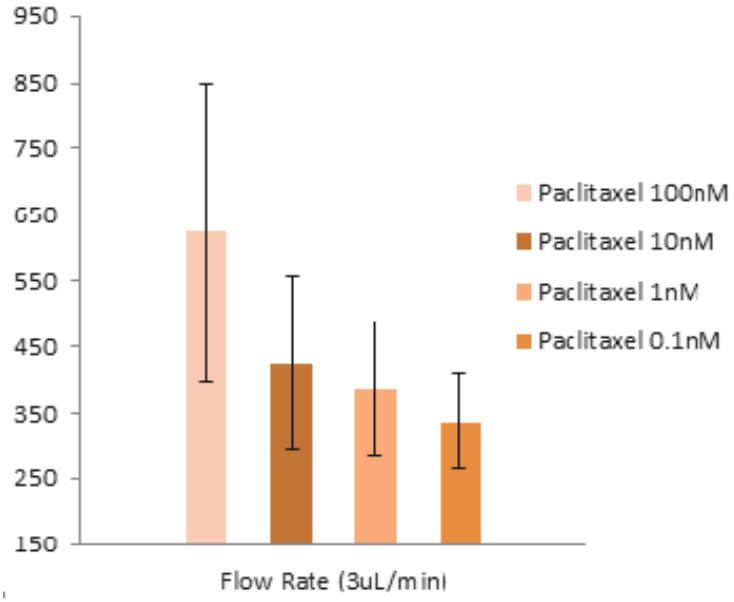

Figure 7 Flow velocity characterization of MDA 231 with different concentrations of paclitaxel

Table 3 Cell adhesion for 3ul/min flow rate for MDA 231 with different concentrations of paclitaxel

Anti-Cancer drug concentration	100nM	10nM	1nM	0.1nM
3ul/min	20	8	1	0

2.4 Discussion

Results obtained from preliminary data indicate some of the key features on how this research could address the behavior of the cancer metastasis. Most significant factors of this experiment process is the Matrigel material which consists of Collagen and Laminin.[7] Matrigel is the substitute of the human tissue used in this process.[8] Collagen has an attraction to the cell matrix since collagen IV has perfect adhere to the cells.

Structure of cells consists of integrins covered by an extra cellular matrix, which consists of α and β chains. There α and β subunits bids each other and crates different types of αβ legends.[9] Integrins carrying α1β1 and α2β1 has more binding capability with collagen receptors. [10][11]

Velocity analysis results using beads and cells demonstrate the difference between with and without integrin collagen interaction, because with polystyrene beads moves higher velocity (980um/sec) comparing to the cells (234um/sec) although the dimensions of beads and cells were almost identical (10um). Meanwhile, higher velocities of cells were demonstrated when mixed with paclitaxel (100uM) as seen in Figure 7.

Results obtained from this data demonstrate the flow velocity effect on the cell attachments in matrigel. Lower the low velocity (MDA 231) has more interaction time with the matrigel and cells causing many cells to attach.

During the flow velocity analysis with MDA 231 demonstrated the flow velocity can be characterized in to two different scenarios as Adhesion region and linear region.

Cells were attached in 2ul/min, 3ul/min and 5ul/min, according to the data obtained in Figure 4. Optimal flow rate 3ul/min since many of the cells attached while flowing at 3ul/min flow rate (20 cells). Due to the higher cell number attachment, 3ul/min flow rate has been used for the data analysis.

2.5 Conclusion

Preliminary results observed will demonstrate the basic concepts to understand the cell separation from a primary location (syringe pump) and attaching on the secondary location. Matrigel coated straight channel behaves as the secondary location (metastasis location) in the above scenario. These particular results are important since no previous simulations were available to simulate and understand the metastasis process.

This research will be more vital in many prospects of future cancer research development process such as: In-vitro Analysis of cancer metastasis , more economical than conventional methods, characterization of the different stages of tumor analysis in order to decide the type of treatment (Ex: chemotherapy, radiation therapy, biological therapy, hormone therapy, surgery, cryosurgery), analysis of different cancer cells types metastases in certain types of organs, flow effect on cancer metastasis.

In-vitro analysis is the one of the vital breakthroughs in the proposed devices, which could take cancer research to address many other contradicting concepts of cancer development.

CHAPTER III

AMMONIA OXIDIZING & NITRATE OXIDIZING ENHANCEMENT

3.1 Introduction

Wastewater management has been significant issue for several decades. Nitrate & Ammonia has been the major concerns in waste water management. Even though biological process has been used during the process growth of ammonia-oxidizing bacteria (AOB) and nitrite-oxidizing bacteria (NOB) has been a major issue due to their slow growth. However the following process will conduct a method of enhancing the efficiency by encapsulating the two bacteria together by the desired proposition, by Polyethylene Glycol Diacrylate (*PEGDA*).

Nitrosomonas europa (commonly known as AOB) is knows as gram-negative chemolithoautotroph that can derive all its energy for growth of oxidation from ammonia to nitrite.[12] This microbe prefers an optimum pH of 6.0-9.0, which is neutral conditions, has an aerobic metabolism and prefers a temperature range of 20-30 degrees centigrade.[13] Due to the large amounts of ammonia this particular bacterium needs to consume for energy to cell division. In this particular scenario, cell division can take up to several days. Ammonium sulfate considered to be the main source of the ammonia in the media and provides the concentration of 50mM of NH_4^+ in the media. Since *Nitrosomonas eurpoea* is an autotrophic nitrifying bacterium, it takes carbon in from the atmosphere through fixation, reduction and incorporation of carbon dioxide. The potassium and phosphorus source is provided by potassium monophosphate in the

media. *Nitrobacter winogradskyi* (commonly known as NOB) is a gram-negative chemolithoautotrophic bacterium capable of extracting energy from the oxidation of nitrite to nitrate.[14] In the absence of nitrite it uses solely carbon sources and acts as a chemoorganoheterotroph. It uses nitrate as an electron acceptor producing nitrite, nitric oxide and nitrous oxide. When oxygen is present it oxidizes nitrite to nitrate. This microbe prefers an optimum pH of 7.3-7.5, fairly neutral conditions, has an aerobic metabolism and prefers a temperature range of 20-30 degrees centigrade. Under optimal condition *Nitrobacter* double every 13 hours. Sodium nitrite is the main source of nitrogen in the media and provides the concentration of 2mM of NO_2^-. Since *Nitrobacter winogradskyi* is an autotrophic nitrifying bacterium, it takes carbon in from the atmosphere through fixation, reduction and incorporation of carbon dioxide.

The nitrifying bacteria have very slow growth rates and sensitive to pH and temperature which makes nitrification process extremely slow and sometimes unsuccessful.[15] This study comprehensively investigated to make the nitrification process more efficient and fast which could possibly be achieved if both the bacteria, AOB and NOB, can work together in a close environment. To create a favorable environment for nitrification, AOB and NOB were encapsulated in the Polyethylene Glycol Diacrylate (PEGDA) gel beads with an expectation for efficient nitrification compared to the suspended ones.

3.1.1 Polyethylene Glycol Diacrylate (*PEGDA*)

Bio-compatibility and diffusivity are vital property when it comes to bio applications. Matrigel, Collagen, Sodium Alginate & Polyethylene Glycol Diacrylate are among the main resources when it comes to bio-compatibility. Each material has their individual properties instead of stiffness and absorbance of liquid. Liquid absorbance & high porosity has been considered for the application of encapsulation.

Polyethylene Glycol Diacrylate (PEGDA*)* has been widely used as a soft gel based material for in vitro cell analysis. Porous structure is supportive for cell encapsulation, tissue engineering, and tissue culture. Tunable physical properties of the structure provided samples to grow by mimic native extracellular matrix (ECM).[16][17] Encapsulation of cell improve the cell performance due to the compact structure allowing more nutrition and ventilation due to the porosity.[18] Mechanism described in this paper explains layer by layer approach for the dual encapsulation. AOB & NOB cells encapsulation by both sides of the structure will allow them to react directly and more efficiently without being scattered in the cell solution. The goals of the research was to compare the two nitrification conditions, suspended and encapsulated, and establish a correlation between the performance of capsulated cell with the nitrification process.

3.1.2 Ammonia-Oxidizing Bacteria (AOB) & Nitrite-Oxidizing Bacteria (NOB)

Nitrification process is the key factor of removing Nitrogen substances from wastewater system. It consists of a two-step process as shown below. Ammonia (NH_4^+) is first oxidized to nitrite (NO_2^-) by ammonia-oxidizing bacteria (AOB), and then nitrite is oxidized to nitrate (NO_3^-) by nitrite-oxidizing bacteria (NOB) (Reaction 2 and 3).

$$NH_2COHN_2 + H_2O + 7H^+ \longrightarrow 3NH_4^+ + CO_2 \quad (1)$$

$$2NH_4^+ + 3O_2 \xrightarrow{AOB} 2NO_2^- + 4H^+ + H_2O \quad (2)$$

$$2NO_2^- + O_2 \xrightarrow{NOB} 2NO_3^- \quad (3)$$

However the above AOB & NOB bacteria should be mixed to a ratio of 2.5:1 ratio in-order to achieve the optimum reaction capability.

3.2 Experimental

3.2.1 Fabrication Process of SU8 2075 Mold

Computer generated mask drawing done using AutoCad, 2012 and printed using the inkjet printer on to a transparent photo mask by Cad Art Services, Bandon, OR at 5000dpi. Conventional lithography process has been used in order to transfer the pattern on to the photoresist.[19],[20],[21] SU8 2075 negative photoresist has been poured on to the silicon wafer and coated using the spin coater. Pattern was transferred on to the cured SU8 2075, using mask aligner. Three separate molds have been fabricated with different dimensions as seen in Figure 8. Figure 8(a) consists of 1mm x 1mm x 300um cubes, Figure 8 (b) consists of 200um x 200um x 300um cubes and Figure 8 (c) consists of 1mm x 1mm x 600um cubes.

Figure 8 SU8 2075 Master molds (a) Bottom layer (b) Middle layer (c) Top layer

3.2.2 Fabrication Process of PDMS Mold

Once the master mold was completed, patterning of the device was done by using PDMS (Polydimethylsiloxane) by using previously fabricated SU8-2075 as a mold on the silicon wafer. Device consists of 3 molds as seen in Figure 8, separately for the bottom layer, middle layer and top layer. Bottom layer was fabricated using conventional process of mixing the curing agent and PDMS prepolymer of SYLGARD 184 Silicone Elastomer Kit, Dow Corning by thoroughly mixing at 10:1 ratio, followed by a backing at 65^{o} Celsius for 2hrs. PDMS mold has been fabricated by Spin-coating premixed PDMS on fabricated device.[22] Middle and top layers has been molded by spin coating premixed polymer at 1000rpm for 4 times and 8 times respectively by baking at 65^{o} Celsius for 1/2hr intervals in-between the each coating. Final backing step was done for 65^{o} Celsius for 12hrs on a flat hotplate prior to the pealing of the PDMS mold. PDMS molding and spin coating steps as seen in Figure 9.

Figure 9 PDMS molding process (a) Bottom layer (b) Middle layer (c) Top layer

3.2.3 Surface Modification of PDMS Mold

By default PDMS mold is hydrophobic once peeled off from the SU8 2075 based silicon wafer mold. It is required to convert the surface in to a hydrophilic surface prior to the experiment as seen in Figure 10(b); PPO solution was prepared with 1% w/v ratio inside DI solution. Once the bottom, middle and top layers were peeled off from the master mold, all the layers were separately treated inside plasma chamber with 5% O2, 25Watt power, and 100mTorr pressure for 30 seconds to make the surface hydrophilic. Polymerized devices were dipped in to Poly (ethylene glycol)-block-poly(propylene glycol)-block-poly(ethylene glycol) with 1% w/v ratio of DI water as a surfactant for 10hrs to in order for the device to be hydrophilic for an extended time.[23]

3.2.4 Dual Encapsulation of AOB/NOB Sample Preparation

Stock AOB and NOB solutions have been centrifuged at 3000rpm for 3 min to separate bacteria from culture media. Separated cells has been mixed with w the solution prepared by 10000MW PEG-DA (10 wt. %) of 1x PBS solution and 1% v,v solution of photo-initiator (1-vinyl-2-pyrrolidinone, 2,2- 2imethoxy-2-Phenyl-acitophenon

solution[24]. Photo-initiator (1-vinyl-2-pyrrolidinone, 2,2- 2imethoxy-2-Phenyl-acitophenon solution works as a UV curable photo agent for the premixed solution.[25] Alignments molds were done under the Eclipse Ti microscope as explained in fabrication process.

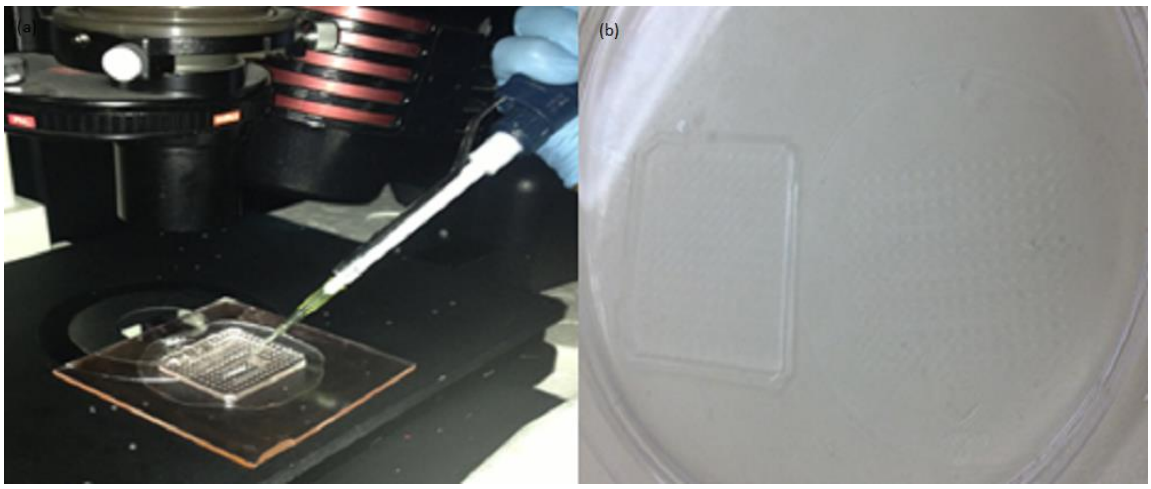

Figure 10 (a) Process of encapsulation (b) Molds soaked in PPO solution overnight for surface modification prior to the encapsulation

3.2.5 AOB/NOB Culture Medium Preparation

AOB culture medium was prepared using a standard recipe of K_2HPO_4 (3.48mg/L), $MgSO_4$ (48.4mg/L), $CaCl_2$(10mg/L), $FeSO_4$(2.73mg/L), Ethylenediaminetetraacetic acid (EDTA- 1.4mg/L), $CuSO_4$($6.40x10^4$mg/L), Na_2MoO_4 (0.0428mg/L), $MnCl_2$ ($7.78x10^{-2}$mg/L), $ZnSO_4$($2.28x10^{-2}$mg/L), $CoCl_2$($5.46x10^{-2}$mg/L). Final measured Ammonia Concentration and carbon concentration of the standardized solution come out to be 20mg/L and 36mg/L. Number of cells inside the cube was estimated by taking the average of cells in several locations of an each sample of sample image, then converting in to the volume of cube size. Washed encapsulated cells and suspended cells twice by above medium without adding ammonia ($(NH_4)_2SO_4$) and carbon (Na_2CO_3).

3.2.6 AOB/NOB Sample Preparation for Encapsulation

Three separate layers with 300um depth squares were placed on a 4"x4" tinted glass slide as seen in Figure 11(b). Curing the PEG-DA premixed bacteria was done as a layer by layer process at a time by using PDMS mold as a curing chamber each time as seen in Figure 11 (a-d). At the begining140ul of AOB solution was suspended in to the bottom chamber and shredded on top of the top layer of PDMS device followed by a UV exposure for 30s with UV lamp (Entela BlackRay B100AP). Once the AOB premixed bottom layer was cured 2nd layer film of was aligned on top of the 1st layer and applied with a thin layer of NOB premixed PEGDA solution of 100uL dispensed and it was exposed to UV for 1min for the curing. Middle PDMA film has been cured once the

curing has done and 3rd top layer was applied on top of the cured middle layer. Alignment of the all layers were done by 5x microscope lens (Nikon Eclipse Ti) and suspended AOB bacteria premixed PEG-DA of 400ul was suspended and cross-linked via UV lamp for 1min. Final structure of schematic diagram as seen in Figure 11 (h).

3.3 Experimental

3.3.1 AOB/NOB Viability Analysis

Since the cross-linking was done using UV light source, it is arguably if the cells were affected by the light source or not. Due to the fact viability test was conducted using Invitrogen LIVE/DEAD® BacLight™ Bacterial Viability Kit was used using the dye SYTO® 9 dye propidium iodide to identify the live and dead cells before and after encapsulation.[26] 1uL of each of both red and green dye has been premixed and sample solution was mixed with 1mL of viability kit and incubated in room temperature for 40mins prior to the imaging. The green color fluorescence represented the live cells and the red color represented the dead cells. The images were then captured by confocal microscope (Zeiss 510 META NLO Multiphoton Microscope). Standard deviation distribution of cell viability was calculated by taking six samples of each data in to account. Test was conducted in 1st day of encapsulation and 7th day of encapsulation to check the cell growth/viability distribution as seen in Figure 12.

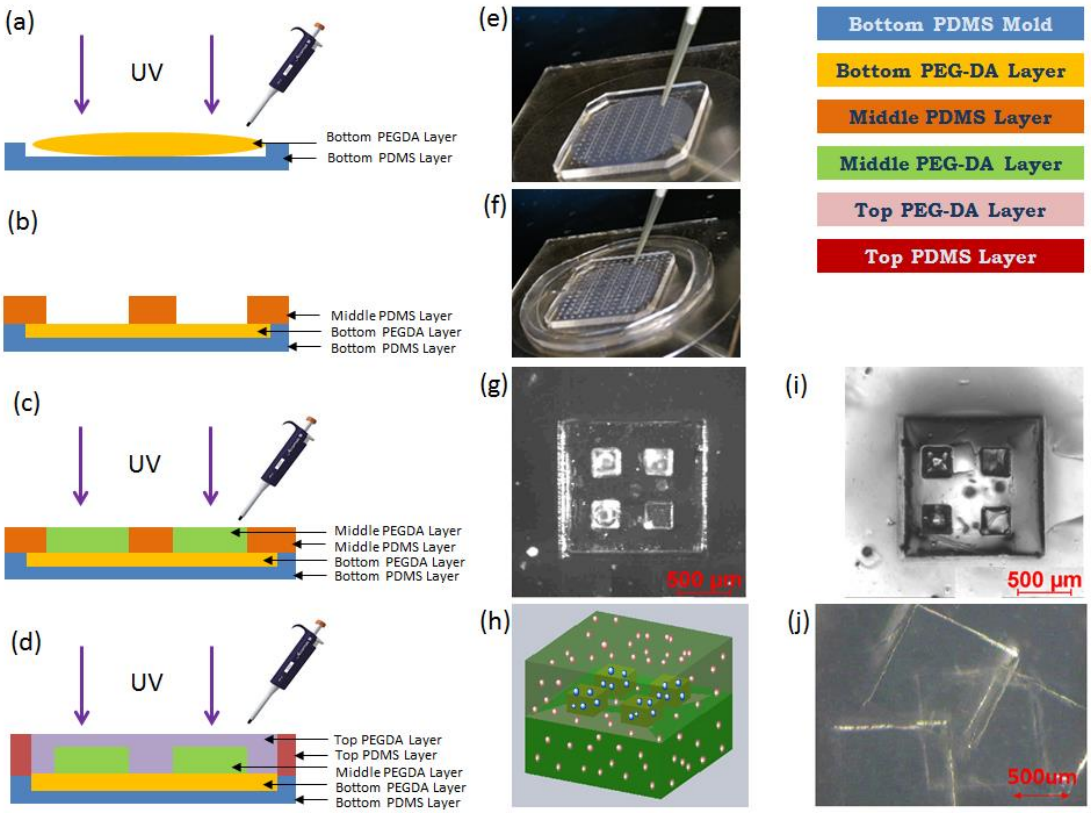

Figure 11 (a) Schematic diagram of PEG-DA cross-linked via 45 second UV exposure, (b) Schematic diagram Bottom PEG-DA cross-linked, middle PDMS Layer aligned with bottom PEG-DA cross-linked layer, (c) 2nd PEG-DA layer dispensed into the pre aligned 2nd PDMS layer and cross-linked via 1min UV Exposure, (d) Schematic diagram middle PDMS layer peeled off, top PDMS layer aligned with 2nd PED-DA Structure. 3rd PEG-DA layer dispensed in to pre-aligned 3rd PDMS layer and cross-linked, (e) 1st layer AOB encapsulation photo, (f) 2nd Layer of NOB pre-mixed PEG-DA encapsulation (g) Fluorescence image (500um Scale bar) (h) Schematic diagram ,(i) Bright field image , (j) Cell encapsulated cubes inside AOB medium (0.7x)

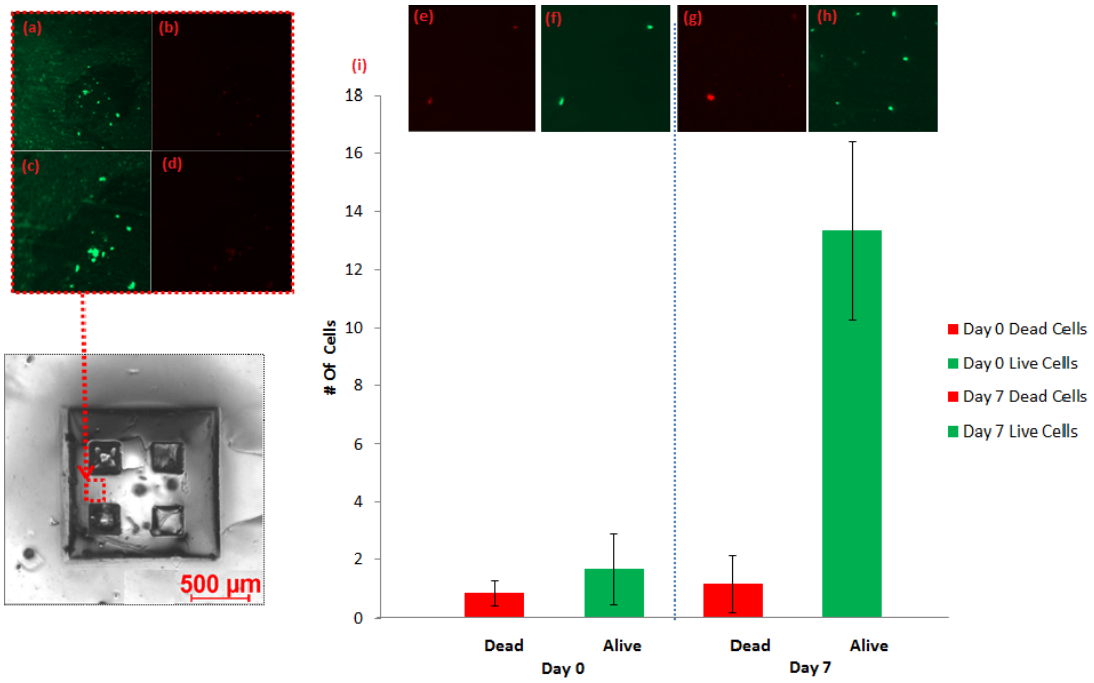

Figure 12 (a) 60x image live cells, (b) 60xImage of dead cells (c) 180x image live cells, (d) 180x image of dead cells, (e) Day 0 dead cells, (f) Day 0 live cells, (g) Day 7 dead cells, (h) Day 7 live cells, (i) Graph of average cell viability comparison of day zero and day 7 after encapsulation

3.3.2 Ammonia Removal Rate Comparison

This particular experiment was conducted by optical measurements and it demonstrated encapsulated ammonia consumption rate was 18.5% efficient than the suspended samples as seen in Figure 17 (a). Experiment was conducted for different samples of blank solution (without samples), different encapsulated capsules of 30, 60 and 120 capsules in 4 separate flasks with 100ml of media in each solution. As seen in Figure 17(b), ammonia decrement in a given period of time increases proportional to the number of encapsulated samples. As seen in Figure 17(b), blank solution sample almost behave as a constant, while 30, 60, 120 samples decays exponentially over the time period.

Ammonia reduction was compared using two methods in order to do a better comparison. In this scenario, both encapsulated and suspended cells was calculated using the standard curve created from the phenate method was measured using both optically using UV spot source by Agilent 8453 UV-visible Spectroscopy System and Ammonia Ion selective electrode of Thermo Scientific, CAT NO 951210 using change in Voltage output over the time period.[27] Both methods were used to compare the results in this experiment. It reveals both results demonstrated identical trends independent of methods.

3.3.3 Long Term and Short Term Ammonia Oxidizing Analysis of Electrode

Both long term ammonia oxidizing analysis and short term ammonia oxidizing was done in order to find the optimum curve. Long term analysis of 48hrs showed a steep reaction curve in the 1st 10hrs of the experiment, as seen in Figure 13(a). Therefor another experiment of short term analysis was done in order to observe the short term analysis as seen in Figure 13(b). This experiment was conducted by the Thermo Scientific Ammonia Ion Selective Electrode. Final Result was calibrated according to the standardized curve.

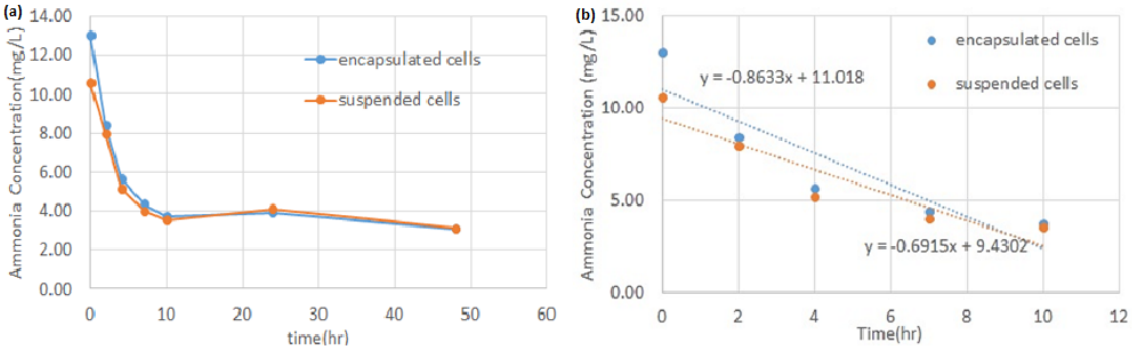

Figure 13 (a) Ammonia consumption rate acceleration comparison over a 48hrs time period, using Probe Analysis. Figure 5(b) Ammonia degradation rate due to AOB, by probe method

3.3.4 Long Term and Short Term Ammonia Oxidizing Analysis of Optical Density

Similar to the probe method, behavioral analysis for Ammonia oxidization was done over a period of 72 hrs as to check the optimum curve as seen in Figure 14(a). Here it demonstrated significant decrement occurred during the 1st 10hrs. Therefore, another analysis was done for the 1st 10hrs as a result as seen in Figure 14(b).

Both conditions encapsulated cells were grown for 7 days until the cells become adaptive and stabilized inside the new conditions. As similar to probe analysis, optical measurements also demonstrated similar trend lines. Ammonia concentration was calculated and normalized using the number of fluorescence for suspended cells and encapsulated cell. In this scenario, Ammonia oxidizing reaction was more efficient once the cells are encapsulated and clustered in to a single cube than scattered samples.

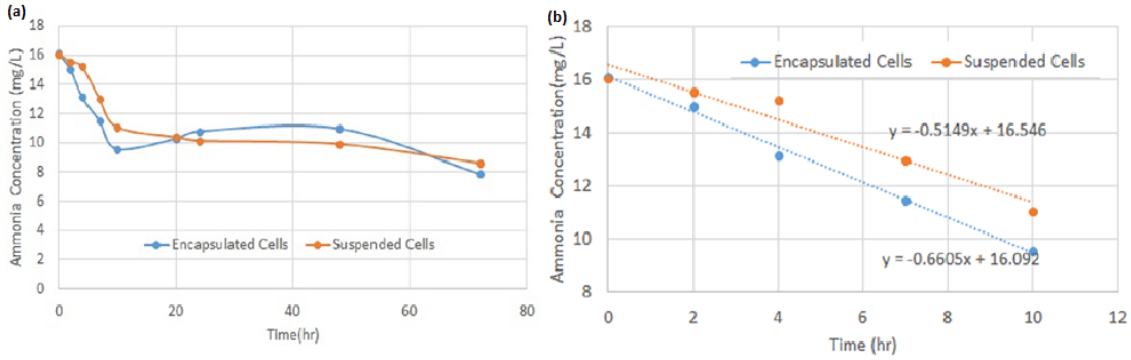

Figure 14 (a) Ammonia consumption rate acceleration comparison over a 72hrs time period, using optical density Analysis; (b) Ammonia degradation rate due to AOB, by Optical density method

3.3.5 Short Term Ammonia Oxidizing Deceleration Rate Comparison for Electrode and Optical Density

Ammonia removal rate per cell in both cases of electrode and probe methods were calculated by considering the rate of change in each slope between data points of Figure 13(a) and Figure 14(b) for the 1st 10 hrs of data. Both cases for encapsulated and suspended cells concentration started with same amount and showed a steep oxidization in 1st 7hrs, and maintained stable scenario from 7th to 10th hrs of data as seen in Figure 15.

As for the Probe method, 1st 4hrs demonstrated a steep deceleration, while reaction minimized from 4th to 7th hrs. As comparing to the probe method, reaction almost became neutral from 7th to 10th hrs of data as seen in Figure 16.

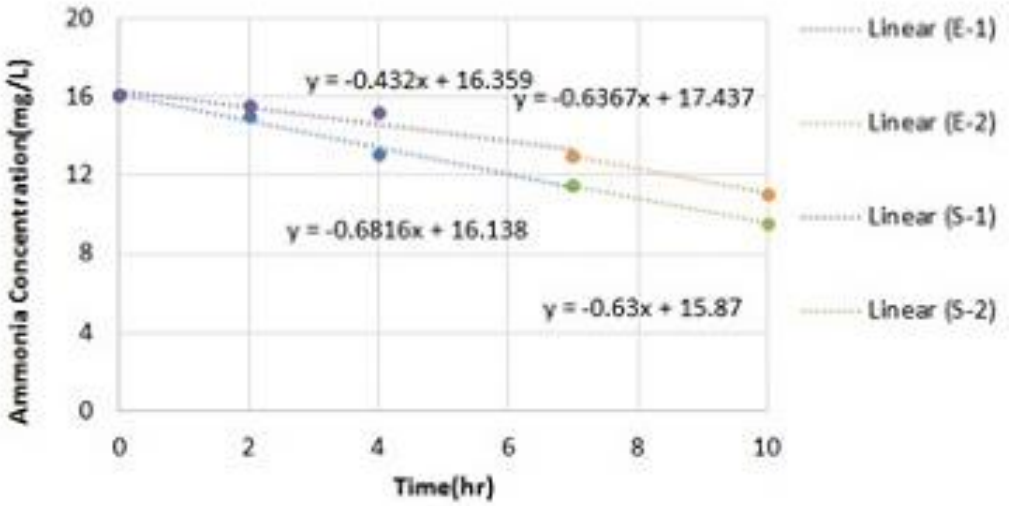

Figure 15 Consumption of ammonia acceleration rate comparison over a 10hrs time period, using optical density analysis

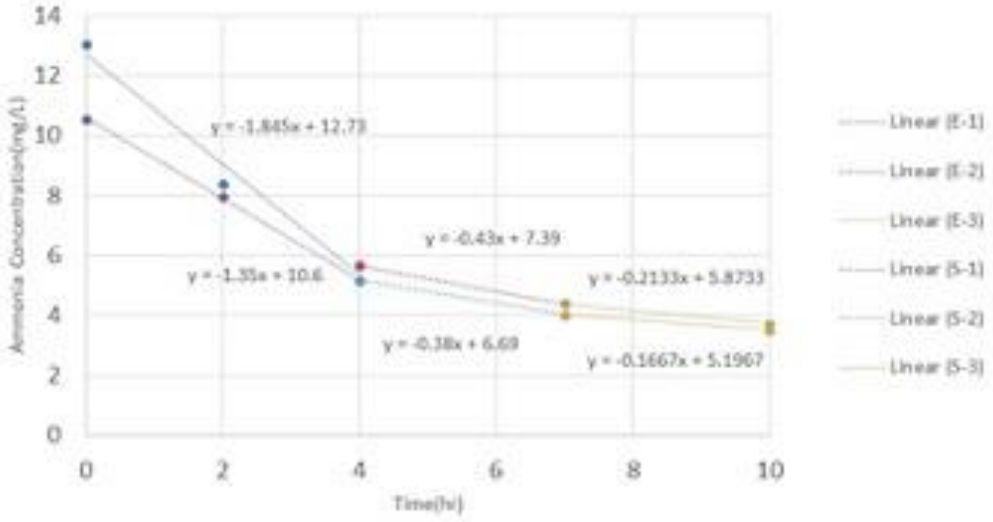

Figure 16 Consumption of ammonia acceleration rate comparison over a 10hrs time period, using Probe Analysis

3.3.6 Ammonia Removal Comparison for Different Concentrations

Experimental Analysis was demonstrated Suspended AOB/NOB and 120 AOB/NOB capsules of same concentration Figure 17(a). At 10hrs encapsulated samples removed almost 45% of Oxidized Ammonia, while suspended samples removed 25% of Oxidized Ammonia. This concludes encapsulated samples works almost 20% higher than the suspended bacteria cells. Particular example demonstrates the encapsulated bacteria works more closely and efficiently as they are more closed and congested together.

Final set of data was calculated for different samples in of 30, 60 and 120 capsules followed by a blank solution of 100ml. 30, 60 and 120 capsules were dipped in 3 different beakers of 100ml in-order to provide the same conditions. Blank solution oxidization remains constant and oxidization rate increases proportionally to the number of capsules as seen in Figure 17(b).

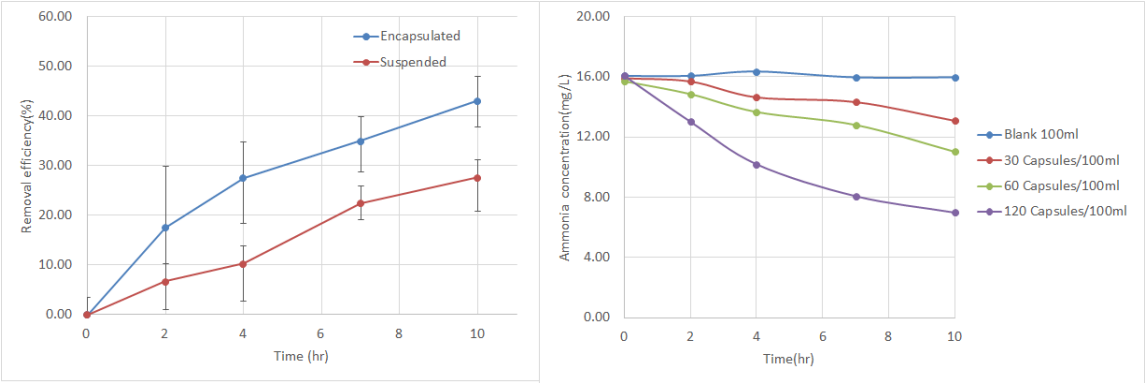

Figure 17 (a) Ammonia removal rate for encapsulated and suspended cells, (b) Ammonia consumption rate comparison for different samples of blank solution, 30, 60, 120 encapsulated

3.3.7 Nitrite Oxidization

Capsules were combined with both AOB and NOB bacteria cells to improve the efficiency. Presence of AOB cells were demonstrated in previous experiments of Ammonia oxidizing, while presence of NOB cells and there functionality is expressed in Nitrite Oxidizing demonstrated in Figure 18. Nitrite to Nitrate was oxidizing was done through encapsulated NOB cells. [28] Blank solution of 100ml media solution used as control, while same amount of NOB/AOB suspended cells and encapsulated cells used for the efficiency testing. Experiment was conducted in a closed environment for all scenarios while encapsulated cells 14-15% efficiency in oxidizing than the suspended bacteria solution as seen in Figure 18.

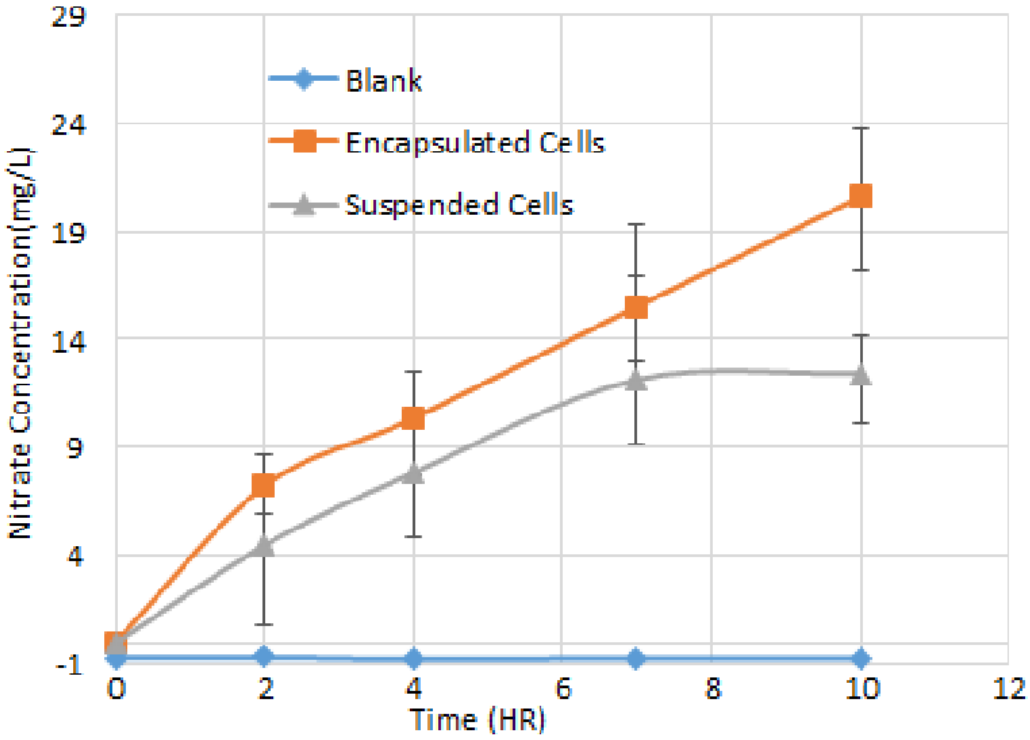

Figure 18 Nitrate Oxidization due to NOB bacteria with respect to time

3.3.8 Ammonia (NH_4^+) Reduction per Cell

Michaelis–Menten kinetics model has been used to calculate the ammonia removal efficiency per cell using the oxidizing data as a bulk sample for calculations. Proximity of number of cells per sample volume of cube has been calculated by the fluorescence dead/alive images taken for the viability data. The ammonia removal rate of one encapsulated bacteria cells demonstrated 10^3 times higher than suspended cell as seen in Figure 19(a) and Figure 19(b).

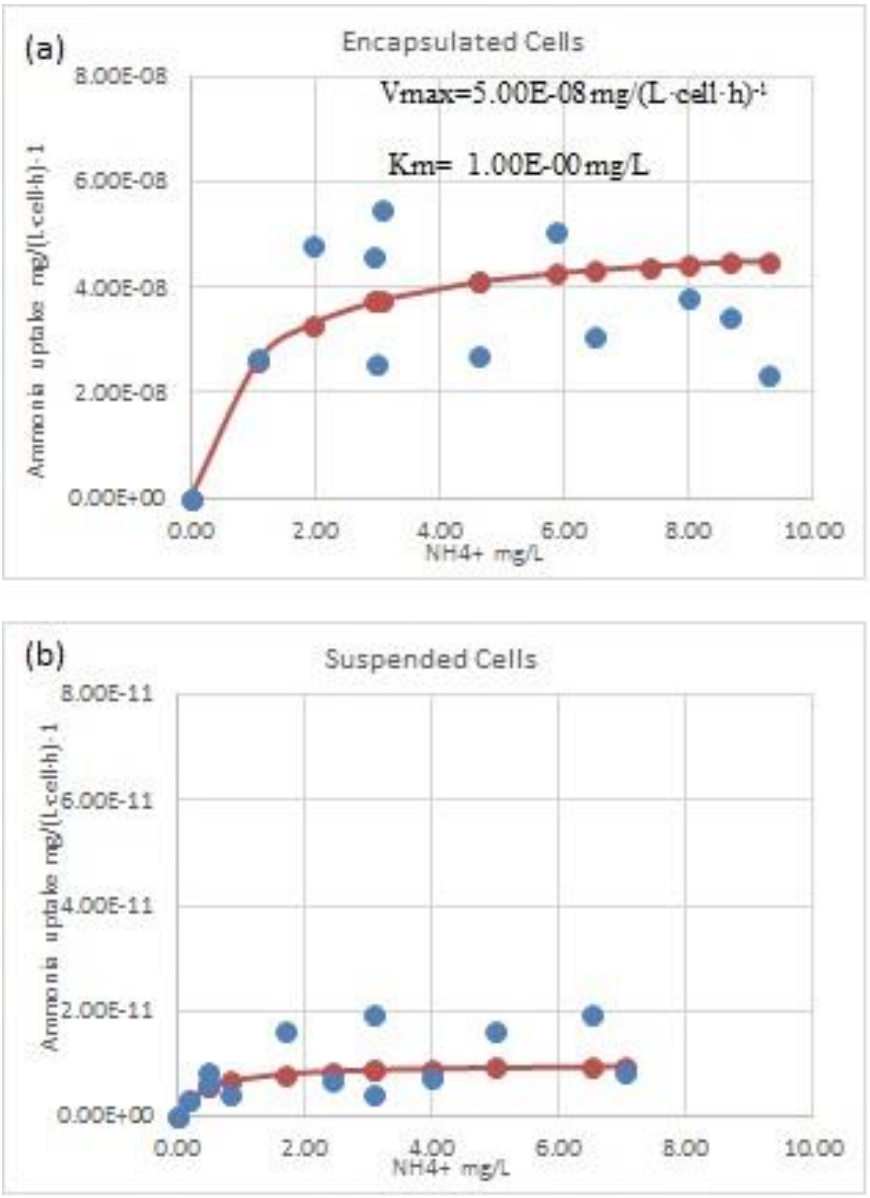

Figure 19 (a) Ammonia removal rate for encapsulated bacteria cells, (b) Ammonia removal rate for suspended bacteria cells

3.4 Discussion

Experimental procedure of AOB/NOB encapsulation was previously limited due to the mass production capability issue. Swelling due to absorption of solution in PEG-DA was another issue that previous researchers have with encapsulation of two types of bacteria. As an example porousness and the young's modulus of PEGDA will vary due to the molecular weight of PEGDA. [29] Eliminating the limitations of mass production of bacteria encapsulation as 3D structures was addressed in the above discussed method.

Meanwhile, there are limitations using different types of material of hydrogel due to the swelling. Since the different amount of absorption hydrogels will expand differently, particular expansion difference will tend to rupture the bacteria and damage the cell structure and they tends to squeeze out of the porous structure due to the internal pressure created by hydration and de-hydration. [30] Using same material throughout will maintain the volume and expansion proportionally without damaging the bacteria. On the other hand bacteria will require moisture and porous structure to remove the waste for the longer survivability. Since PEGDA 10000MW can hold more moisture, this limitation will be eliminated using this particular technique.

Design of the particular dual encapsulation structure provides the complex nitrification process in to a simpler sequential step by step scenario. Basically the process of Nitrification starts from AOB and final Nitrite to Nitrate process is done via NOB. [31] As seen in structural Figure 11 (h), AOB is wrapped outside of the NOB islands of quarto blocks providing oxidization simplicity from outside to inside. Since the AOB is exposed to the outside and NOB is exposed to AOB by encapsulation in

inside it sophisticated structure will provide more simplified value to the Nitrification process. Non-toxicity of the PEGDA hydrogel material and environment friendliness, than the other bio-hazards water purification methods will provide more value to the above method in future applications of water purifications.

3.5 Conclusion

Waste water management has gone through several advance procedures in past decades since the industrial revolution. Basic idea of this particular method will provide less bio-hazardous method of water purification process. It is proven by different scenarios that above method of dual encapsulation performs much higher efficiently rate than the standard premixed AOB/NOB bacterial solutions. This method addresses the higher growth efficiency growth rate of bacteria due to encapsulation, since growing NOB is been a more difficult task by balancing its PH sensitivity.

One of the major contradictions of the above method would be the viability and functionality of bacteria after UV exposure, since UV denatures cell growth factors. However, the Dead/Alive viability data proves cells gain more exponential growth even after exposure to UV. Method of encapsulation of AOB/NOB by PEG-DA hydrogel becomes more practical approach in the nitrification process due to the porous structure in the soft hydrogel material. It provides an environment for the cells to grow and gain it’s oxygen for the oxidizing process via the 2-3um range porous structure in the hydrogel applicator.

CHAPTER IV

MAGNETIC LOCOMOTIVES AND RESPONSE OF MAGNETIZED C-ELEGANS

4.1 Introduction

Nematodes such as zebra fish and c-elegans (caenorhabditis elegans) have been one of the major aspects among biologists in the recent past decade. Still it's in development stage although some researchers have found methods to analyze their behavior, mussel movement and internal organ observations using conventional microfluidic techniques. Researchers have spent more time in analysis of c-elegans since there are future applications such as processing neural networks and treating drug delivery system in the future potential applications by using these nematodes. Recent experiments have focused on the mechanical properties of c-elegans. In this particular experiment it discuss about how to control steering of c-elegans and locomotion due to magnetic loads by using c-elegans.

4.1.1 Introduction to C-Elegans

C-Elegans is a type of transparent species which is about 1-1.5mm in length. [32] They are categorized as a type of nematode species which stands for round warms. Initial egg stage of the c-elegans starts from hatched egg stage consisting of 600 cells and grows in to a grown species over the time period. [33] Growth of the c-elegans is based on an agar plate consuming E. coli strain OP50 bacteria as food on a Nematode Growth Medium (NGM) based medium. [34] Nematode growth media is buffer solution mainly consists of different types of components pacifically has balanced PH sensitivity of 7.3. Buffer media mainly consist of NaCl, MgSO4, CaCl2, KPO4 and DI water. [35] Life span of this particular nematode is about 2-3 weeks, while 3-4 days between eggs to hatched stage. [36] In-terms of lengths it grown from 200um – 1500um over the time, with cross sectional diameter varies from 10um – 70um. [37] Predictable shorter life span of these species provides the scientists to observe their changes over the lifespan.

4.1.2 Magnetic Nano Particles

Magnetic nano particles has been developed over the period of time and particular types such as turbo beads azide has developed in to small dimensions such varies from 30nm-50nm particle sizes (sigma-Aldrich). Applications of magnetic nano particles include bio-medical applications, water purifications, and palladium catalysis. Due to the injecting convenience and functionalizing capability of nano particles, it has been applied in to vast variety of bio applications of living animals such as feeding

mammalian related experiments. [38] [39] Magnetic nano particles have been used as a source to feeding c-elegans nematodes, in this particular mechanism.

4.2 Experimental

4.2.1 Magnetic Nano- particle encapsulation inside PEGDA cubes

Conventional lithography process of pattern molding using SU8 2075 photoresists has been used to fabricate the master mold of the squares patterns. Photoresists has been spin coated at 1500rpm to create the even layer of thickness. Once the SU82075 becomes cured after the prebaking, pattern was transferred on to the cured layer via 14mW/cm^2 UV lamp. Then the mold was developed inside SU 8 developer, followed by the required post exposure baking. [40]

Prepared structure of hard backed SU8 2075 was used as a mold to create the required PDMS mold. PDMS mold was created after adding 15grams of prepared pre-polymer of 10:1 ratio with curing agent on top of the mold and curing the structure at 65^{o}C for 2hrs. Once the mold was peeled off it can be seen as a hollow structure of PDMS as seen in Figure 20 (a). Surface modification was done for the PDMS layer prior to the experiment and was dipped inside PPO solution for 12hrs to make the structure permanently hydrophilic. All the solution will be directed inside in to the cavity without leaving solution outside by making the structure hydrophilic.

Turbo beads of 0.05g with 1mL of PEGDA mixed with 10uL of photo initiator have been mixed together to as the solution. PDMS mold was placed on a glass slide and 60uL of premixed magnetized PEGDA was injected inside in to the mold. Excessive

solution has been squeegeed using a flat plastic and exposed in to 1.5mW/cm^2 lamp for 45seconds to make it cross-linked. Schematic diagram of cross-linked magnetic beads can be seen in Figure 20(b).

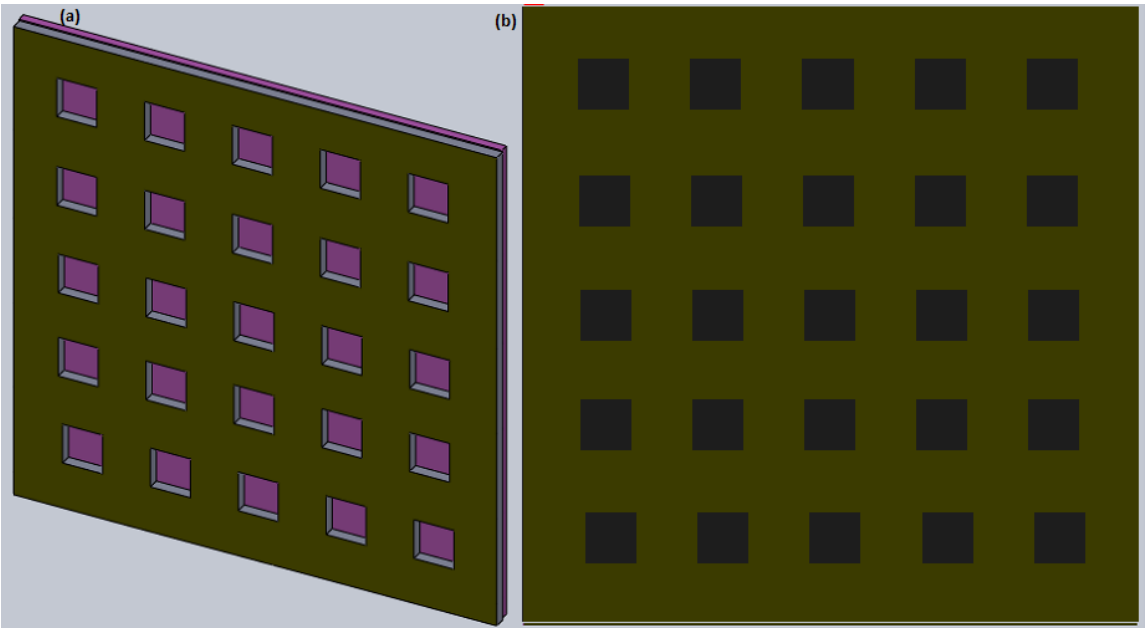

Figure 20 (a) Hollow structure of PDMS layer after peeling off from SU8, (b) Cross-linked PEGDA mixed turbo beads inside the PDMS structure.

4.2.2 Magnetizing C-Elegans

Magnetizing the c-elegans was done by mixing the magnetic nano particles with their food. Turbo beads Azide with 30nm-50nm were used as the magnetizing source to mix with their food source e-coli. Since c-eligans is able to distinguish the beads from e-coli, it is necessary to do the surface modification for the magnetic beads to attach with the food. Poly-allylamine hydrochloride (PAH) has been applied with the magnetic coating to make the positive charging layer to apply with e-coli negative charge layer. [41] [42]

Two day synchronized c-elegans from a beached sample has been used for the particular magnetizing process, since they are able to consume food and deposit magnetic particles on their body. Fresh c-elegans were harvested without food inside an agar plate for 24hrs prior to transferring on to the food plates. 10mg of turbo beads were vortex mixed with 100ul of PAH solution for 30mins prior to mixing with the food. [43] Then the prepared turbo beads were mixed on a plate shaker at 400rpm for 1hr at room temperature inside a dark room with 300uL of OP 50 e-coli strain. Mixing procedure will allow e-coli to be attached properly by bombarding in to the positively surface coated magnetic nano particles.

150uL Premixed nano-baits were then applied evenly on to an agar plate to make a lawn of e-coli bacteria. [44] E-coli were allowed to grow for 24hrs and attached to the agar plates prior to the transferring the fasted warms. Once the worms are transferred they were fed with nano-baits for 4-5days in-order to grow in to medium size adults and consume sufficient amount of food with magnetic nano particles.

4.3 Results

4.3.1 Magnetic Response of C-Elegans

Magnetic particle swallowed c-elegans were planted on the agar gel plate surface to demonstrate the magnetization. C-elegans was able to slide and attract towards each other in to a pile as seen in Figure 21. Nematodes were suspended on to the agar plate in this scenario. Suspended c-elegans were observed by optical microscope (Nikon Eclipse Ti) in order to capture the time lapse images.

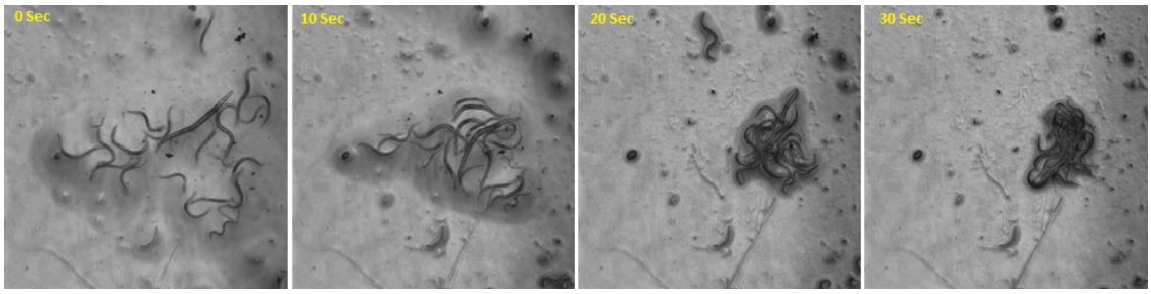

Figure 21 Time lapse image of c-elegans attraction due to magnetic beads inside the body

4.3.2 Magnetic Attraction Towards the Magnetized PEGDA Block

PEGDA hydrogel blocks were separately fabricated by a PDMS block as a template. This particular experiment was done inside the PBS to give them more freedom to move inside the liquid. According to the results shown in Figure 22, it reveals that c-elegans is magnetized to response and attach towards a magnetized particle block.

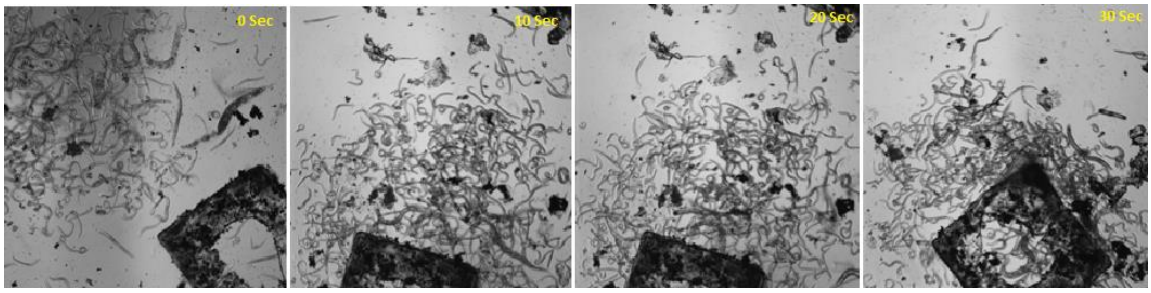

Figure 22 Time lapse image of c-elegans attraction due to magnetic beads inside the body

4.3.3 Magnet Particle Attachment on Agar Plate

Although c-elegans won't have much grip inside liquid due to friction, on agar they have more control over their body by grabbing the agar gel. Friction helps them to manure by avoiding the obstacles. This particular experiment was conducted to see how 1um magnetic beads can attach to their body inside agar plate. Beads were coated on to their body due to the magnetic capability, once they move through the magnetic bead sprinkled path as seen in Figure 23.

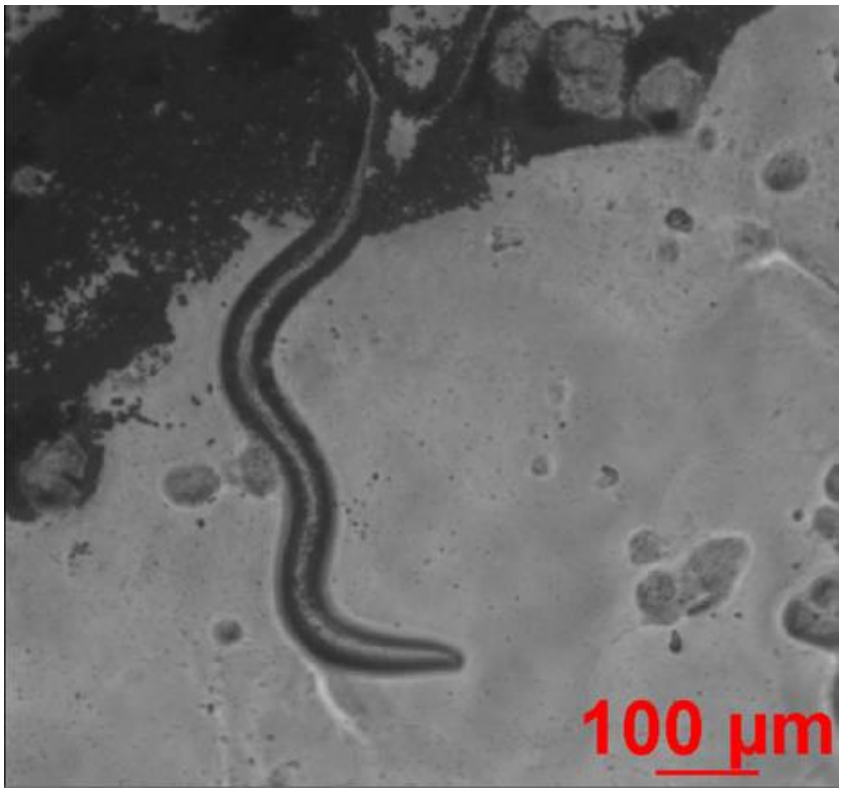

Figure 23 10um bead coated on magnetized c-elegans

4.3.4 Variable Magnet Response to C-Elegans Moving Direction

Magnetic field has been applied via a voltage controlled solenoid variable magnet. Magnetized c-elegans was deposited on to the agar gel. As the voltage increases c-elegans moved away from magnetic field to avoid the obstacle. They have a higher gripping capability and mobility inside agar gel due to the friction. [45]

As seen in Figure 24, movement of c-elegans can be controlled by changing the DC voltage to the magnet. Magnetic-field of the solenoid increases proportionally to the voltage. With the increase of magnetic-field nematodes increases their angle of movement direction increases as seen in Figure 24.

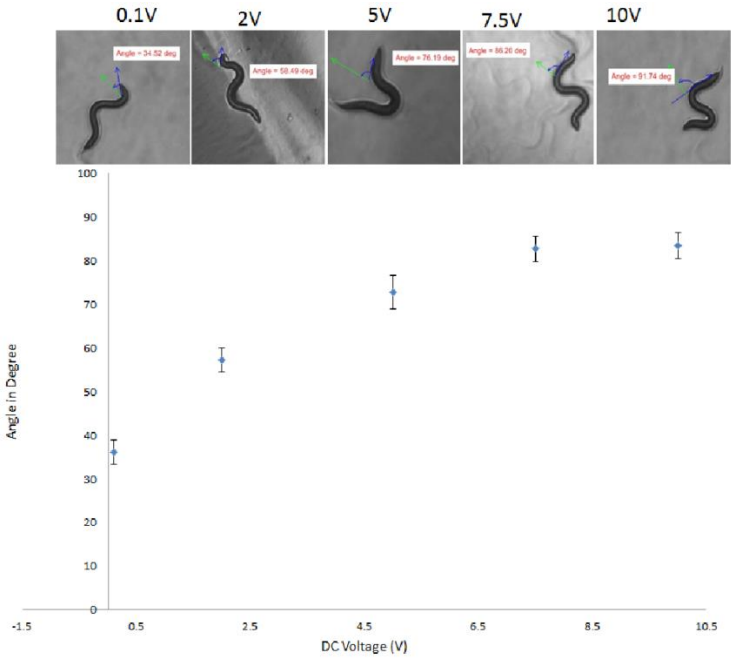

Figure 24 Magnetic field voltage response with moving angle of c-elegans

4.3.5 Encapsulated Magnetic Particle Response

Magnetic nano particles were encapsulated with PEGDA pallets using the mold as seen in Figure 20(a). Fabricated pallets were tested for their ability to movement as seen in Figure 25. Niobium magnet was placed diagonally to the pallets and tested for their movement velocity in PBS (Polly Buffer Saline) based solution. They were able to move 1mm diagonal line within 0.4secons. Testing done using the nano-beads encapsulated in PEGDA demonstrates the particles are capable of responding to the external magnetic field.

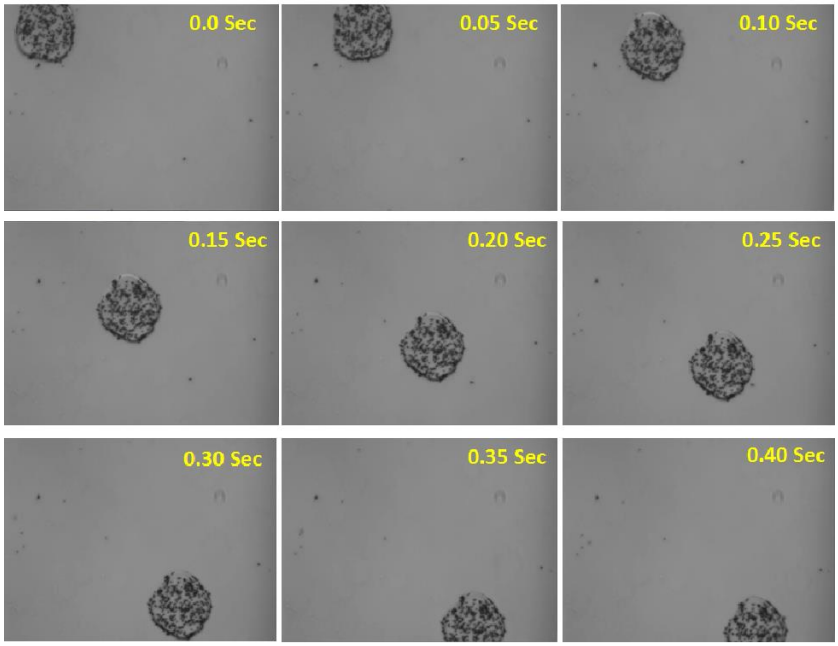

Figure 25 Magnetic field voltage response of magnetized PEGDA

4.4 Discussion

This particular experiment was conducted to demonstrate how to attach external elements to the living c-elegans how as a mechanism of changing moving direction of c-elegans without any contacting external force. Researchers have demonstrated the low Reynolds number able to help c-elegans to move on the surface. [46] Due to the fact moving their direction from a gripping high friction surface such as an agar surface it bit of challenging. Typical growing source of the c-elegans is NGM based agar gel during the life cycle. [47] Meanwhile, c-elegans future development involves drug delivery inside the human body. Above method of attaching the load to the c-elegans will move the approach step ahead helping the future biological approaches.

Changing the moving mechanism and direction of c-elegans has been developed using electric fields. [48] Drawback of using electric field is it's a bi-directional approach such as moving towards negative or positive charge. Magnetic field will give more moving options by using several electromagnets in future applications over the electric field. Since the organs of this particular nematode are covered by a very sophisticated fragile tissue, using an external force such as a tweezers could harm their organs. By using a non-harmful force such as a magnetic field to control their movement it will allow the researchers to handle them without any damage to their organs.

4.5 Conclusion

Drug delivery mechanisms and neuron circuitry building has become a common research topics in this decade. Researchers are seeking in to more capabilities of living resources such as c-elegance and zebra-fish to address above topics. Approaches addressed in this chapter will conduct future approaches in the research developments. Future developments of adding attaching loads to the c-elegans can be used as a source of delivering drugs in to the human body, since the nematodes are known to be non-toxic for humans. Cancer drug delivery is a vast area which still having issues with delivering target drugs in to the tumors. Above approach can be used as a mechanism of delivering appropriate dosage of drugs on to the target cells without damaging the healthy tissues. Magnetic response to change the moving direction and angle will help to guide the c-elegance without harming the drugs and more safely inside the human body in future approaches.

CHAPTER V

PEGDA HYDROGEL ENCAPSULATION

5.1 Introduction

Hydrogel based encapsulations are vastly used in many biological applications such as cell culturing, tissue engineering due to their bio-compatibility, porous structure and high liquid absorbance. Individual characterization differs from application; therefor researchers are using different types of hydrogels such as: collagen, Sodium Alginate and PEGDA for various applications. PEGDA has been a type of hydrogel that has been used since there are number of molecular weights to choose from according to the stiffness and porous cavity size required for the research application.

5.1.1 PEGDA 10000MW Hydrogel

PEGDA hydrogel is a power based which is synthesized from PEG. PEGDA differs from their molecular weight; smaller molecular weight has less porous structure and high stiffness while higher molecular weight has high porous structure and less stiffness.[49] [50] [51] Due to the variable characterizations, PEGDA has become a more versatile applicator in tissue engineering. Preparation was done as Appendix A.

5.1.2 PEGDA Microspheres

Microspheres based on hydrogels are mainly prepared via microfluidic channel interface due to the fragile structure and complexity. Preparation complexity arises when it comes to cross-linking. It is necessary to do within a shorter exposure time; hence the

uncross-linked spheres will create a gulp inside the collection chamber. Size of the microsphere is primarily controlled by the flow velocity, while the maximum size can be controlled by the aperture of the pinching area. Controlling the spherical size is vital since bigger spheres will become out of shape in to a pancake shape elliptical structure once cross-linked.

5.1.3 Fabrication Process Microsphere Device

Fabrication process of PEGDA microspheres was done using conventional lithography process. Negative photoresist SU8 2075 has been used in the process. Once the prebaking was done, pattern shown in Figure 26(a) has been transferred via UV exposure on to the prebaked device. Pattern consists of 3 aperture diameters of 30um, 50um and 100um sizes. Pattern transferred to Si wafer was developed and posted exposure baked at 65^{o}Cfor 5 min and 95^{o}C for 15min in-order to make the pattern stiffer. Finally the PDMS mold was fabricated using SYLGARD 184 Silicone Elastomer Kit with curing agent at 10:1 ratio. Devices were then plasma treated and bonded on quartz cover slip.

5.1.4 Fabrication Process of PEGDA Micro Bullets

Instead of a photoresist master-mold, milling machine fabricated Aluminum master-mold has been used in this process as seen in Figure 27(a). Mold was then fabricated with PDMS using SYLGARD 184 Silicone Elastomer Kit with 10:1 ratio of curing agent as seen in Figure 27(b). Prepolymer fabricated metal mold was then backed at 65^{o}C for 2hrs, and then removed the PDMS layer as seen in Figure 27(c).

5.2 Experiment

5.2.1 PEGDA Microsphere Generation

Microsphere generation typically done using microfluidic device such like a flow focusing mechanism in most scenarios. [52] Although mostly chemical cross-linking has been done in several occasions, UV cross-linking is vital due to the scattering. [53] Scattering effect was overcome by using a photo mask at the bottom of the exposure area while using a thinner glass slide for the most UV absorption in to the PEGDA microspheres. Device fabrication was done using conventional lithography for molds with 3 different aperture sizes. 100um, 50um and 30um aperture diameter devices have been used for the following application, as seen in figure 26. Different aperture sizes of the flow focusing devices able to produce microspheres with maximum sizes of aperture size.

PEGDA microspheres were generated by injection of 40%w/v ratio with mixed DI water and 2% span 80 mixed mineral oil were injected from one side of the flow focusing microfluidic device as seen in Figure 27. Spheres will become stiffer by using high weight to volume ratio of PEGDA and span 80 will perform as a surfactant without mixing oil PEGDA layer. [54] Spheres were cross-linked by using an inverted spot focusing UV light source from the bottom of the chip.

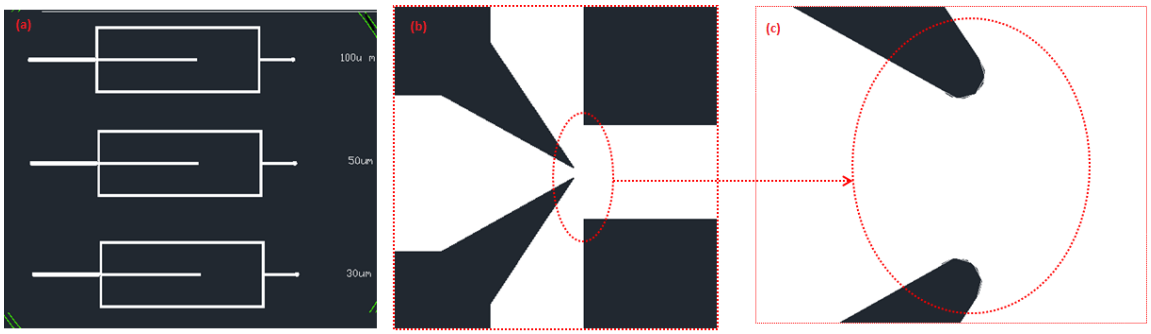

Figure 26 (a) Flow-focusing designs for 30um, 50um, 100um, (b) Aperture area of the flow focusing device, (c) Zoomed aperture area of flow focusing device

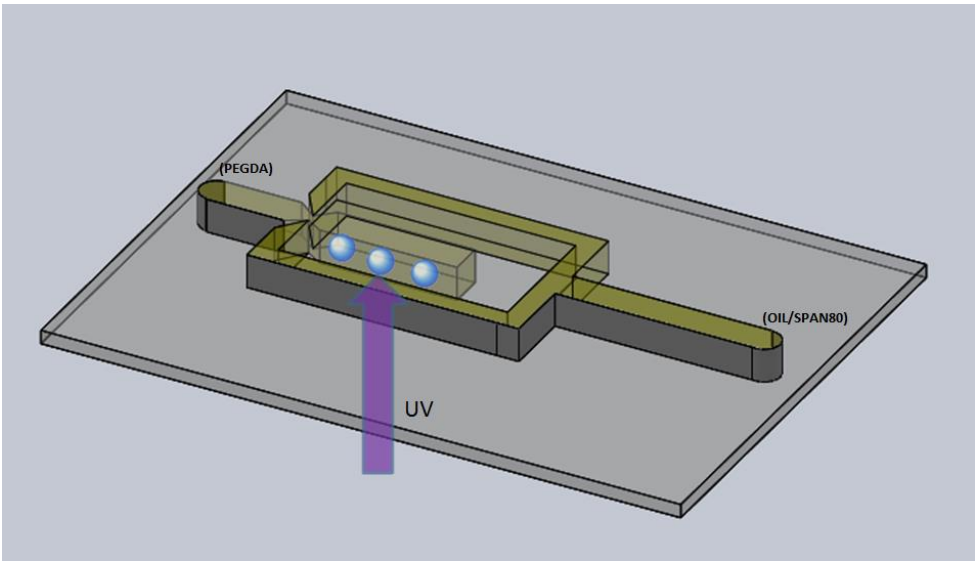

Figure 27 Microsphere generation with flow focusing device

5.2.2 Micro-Bullets Fabrication with PEGDA

Metal mold has been used as the primary mold in this particular scenario as seen in Figure 28(a). Secondary mold has been fabricated by pouring PDMS on to the metal mold and curing at 65^{o}C for 2hrs until polymer become solidified as seen in Figure 28(b). Once the mold become solidified and cured, PDMS mold has been removed and used as the molding device. Bullet fabrication was done using the PDMS mold as seen in Figure 28(c). PEGDA based solution mixed with 1%v/v ratio of photo-initiator. This process can be applied in cell encapsulation; following application has been used to encapsulate bacteria.

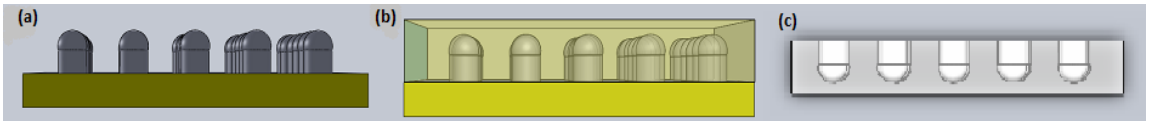

Figure 28 (a) Metal bullet mold, (b) PDMS cross-linked Metal mold, (c) Removed molded PDMS structure of bullet mold

5.3 Results

5.3.1 PEGDA Microspheres

Microspheres were generated and passed through the channel in to the collection chamber. Image of microsphere 30um channel microsphere generation at outlet is shown in Figure 29. Different flow rates of oil/Span 80 and PEGDA/photo initiator were tested in order to find the optimum parameters for the experiment for both scenarios of 50um and 100um aperture sizes, Oil 1.0uL/min PEGDA 1.5uL/min for the 50um aperture diameter. Oil 1.25uL/min PEGDA 2.5uL/min for 100um aperture diameter came out to be the optimum conditions.

Stability of spheres were calculated for the different conditions for 40mins, since it requires a long term flow to get a high yield of spheres for data due to the optimum conditions.

For the 50um aperture channel flow rates follows as:

- Low Limit PEG 0.5uL/min & Oil 1.5uL min
- Upper Limit PEG 1.0uL/min & Oil 1.5uL min

For the 100um aperture channel flow rates follows as:

- Low Limit PEG 1.0uL/min & Oil 2.5uL min
- Upper Limit PEG 1.5uL/min & Oil 2.5uL min

Higher the limit will cause spears bumping in to each other creating an unstable flow and lower the limit will have an unstable flow pressure causing the flow to be interrupted causing the elliptical shape and following generated spheres closer is another issue with

this particular channel. As for the characterization elliptical shape will occur with high unstable flow rates.

For the 50 um aperture channel elliptical shape occurs at flow rates of:

- PEG 1.25uL/min & Oil 1.5uL min
- PEG 1.5uL/min & Oil 1.5uL min

For the 100 um aperture channel elliptical shape occurs at flow rates of:

- PEG 1.25uL/min & Oil 1.5uL min
- PEG 1.5uL/min & Oil 1.5uL min

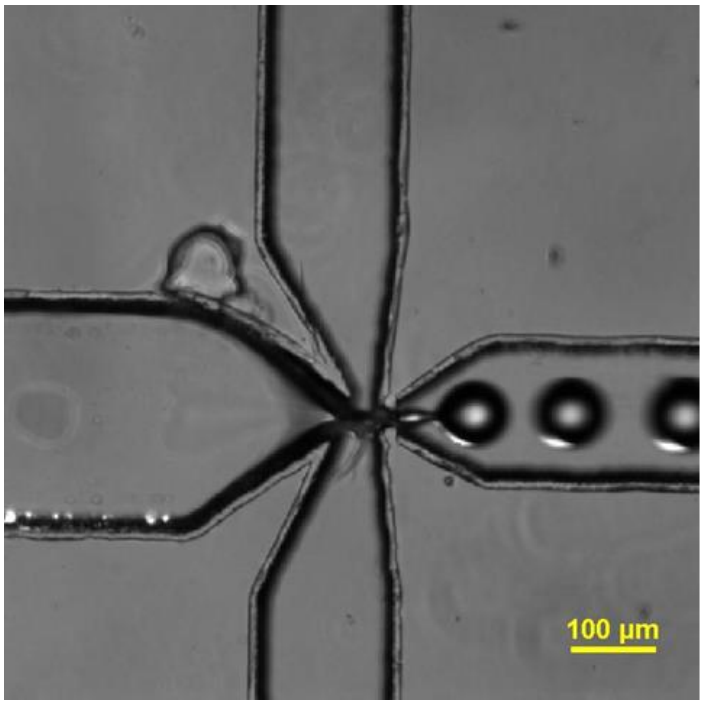

Figure 29 PEGDA microsphere generation from 30um microfluidic device

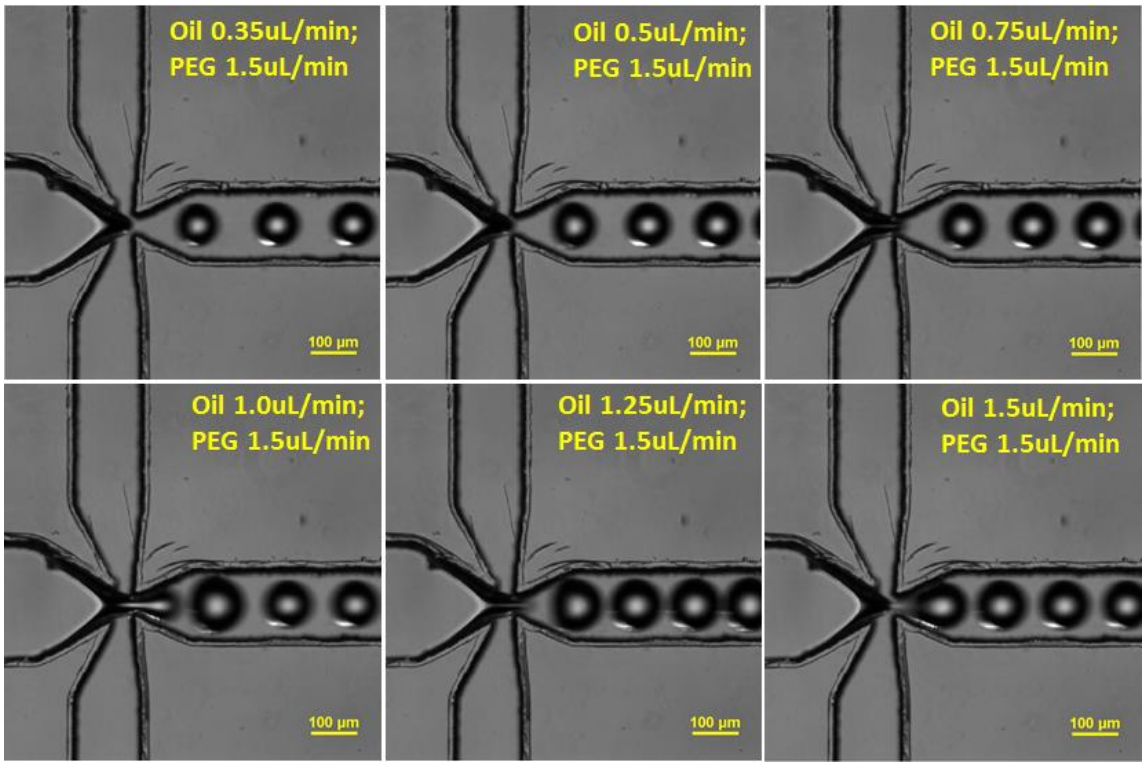

Figure 30 PEGDA microsphere generation from 50um microfluidic device, with different flow rates

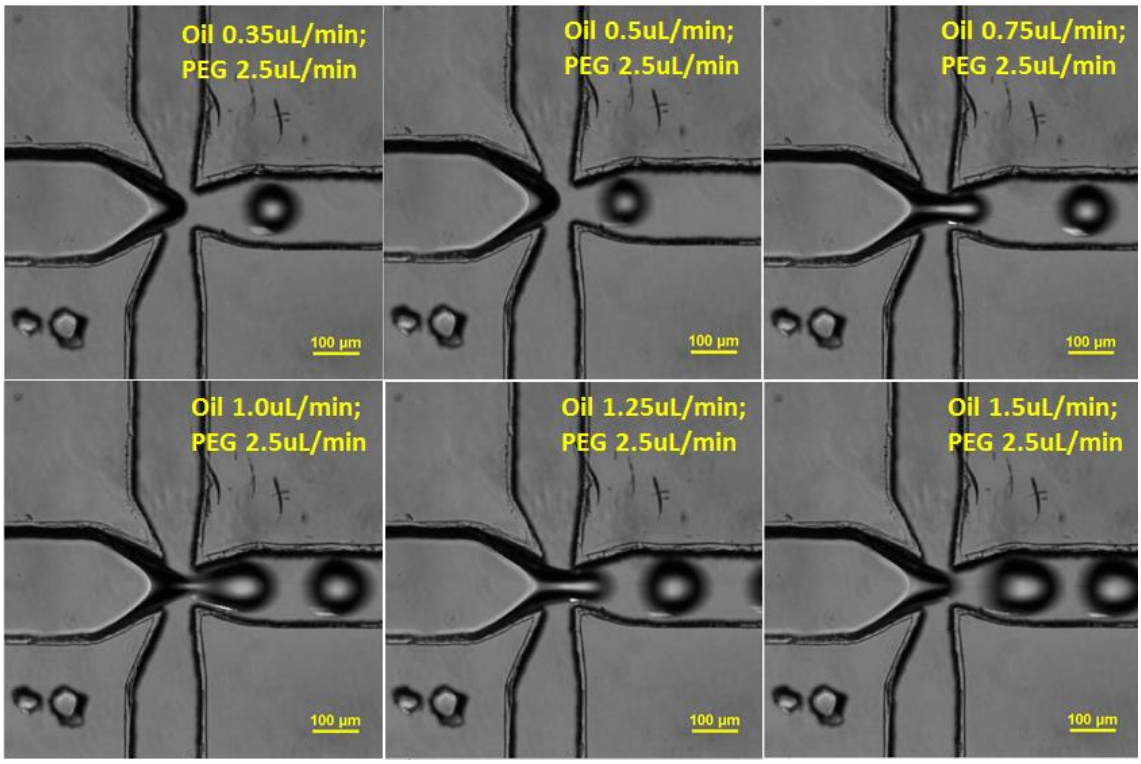

Figure 31 PEGDA microsphere generation from 100um microfluidic device, with different flow rates

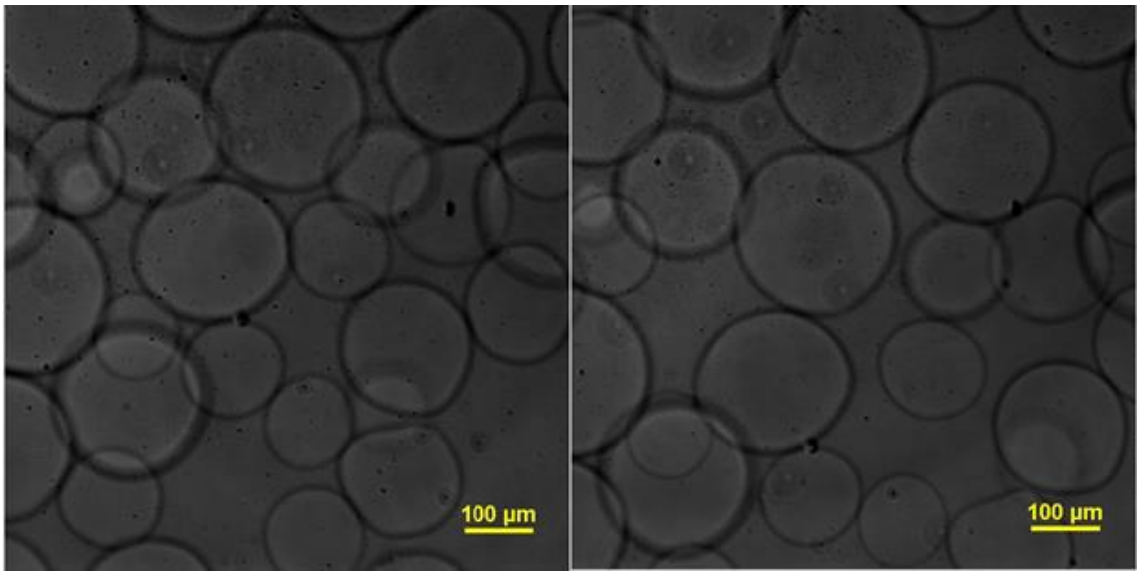

Figure 32 UV cross-linked PEGDA microspheres

5.3.2 PEGDA Micro-Bullets

Micro-bullets were fabricated using the aluminum mold in Figure 28(a). Bullets were in size of 900um and they were tested the liquid absorbance capability. Main purpose for the testing was to encapsulate bacteria cells harvesting. DI water was used in this particular scenario, and it demonstrated a ±250um in size with the DI water as seen in Figure 34.

Bullets were fabricated with AOB bacteria as seen in Figure 33 (a) and tested for the long term survival capability inside the culture medium. Cell encapsulated micro-bullets were able to keep the molded shape as seen in Figure 33(b) and Figure 33(c).

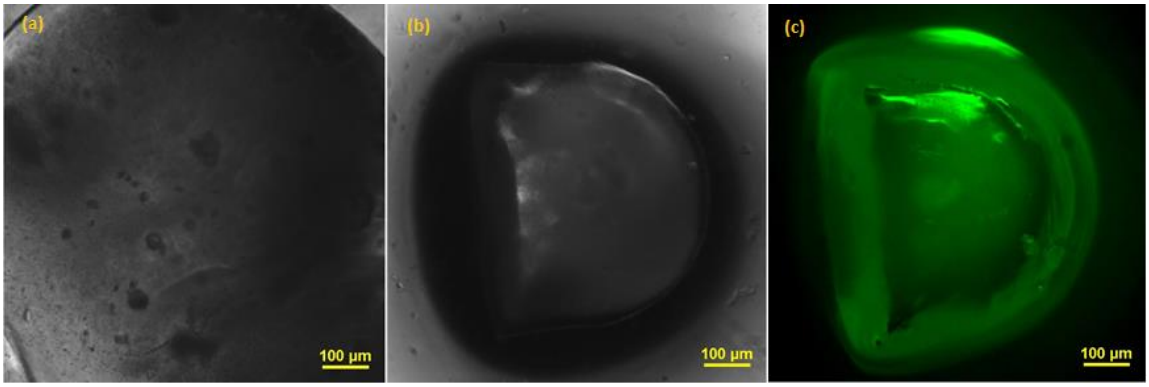

Figure 33 (a) 10x image of micro-bullet, (b) 5x bright field image, (c) 5x bright field contrast image

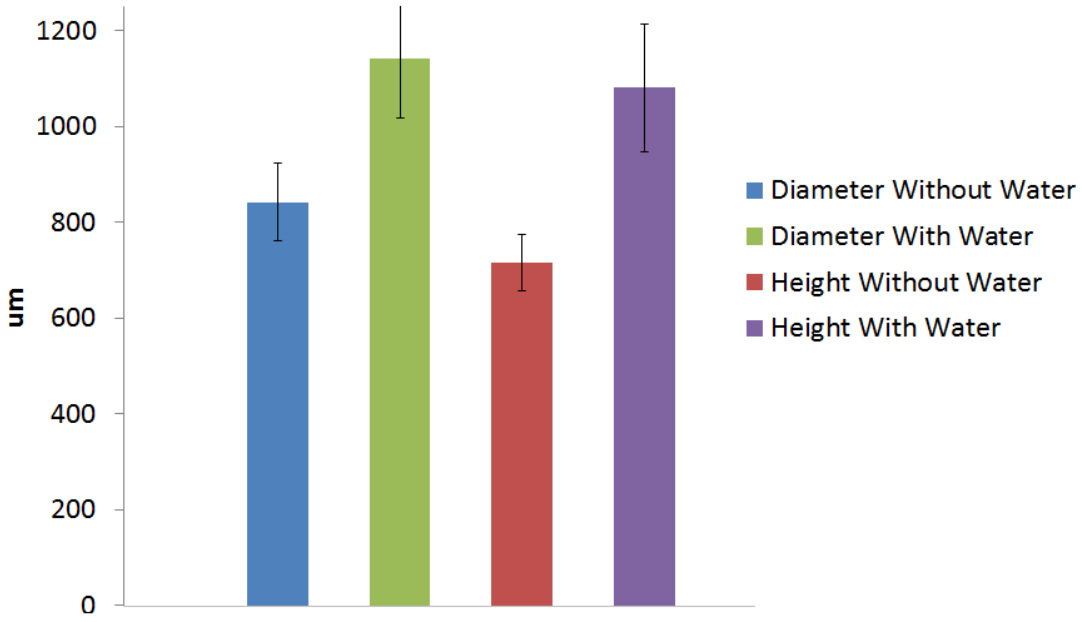

Figure 34 PEGDA micro-bullet swelling characterization due to DI water absorbance

5.4 Discussion

Optimum flow rates are vital in PEGDA microsphere conditions, since it's required to have a constant gap between the spheres due to the bulk cross-linking. If two spheres pass the spot together it will cross-link several spheres together and create a clog in the channel. According to the characterizing, optimum flow rates it requires a UV exposure time of 175us, which provides adequate amount of time to cross-link. As for the elliptical state of spheres, it occurs at above the optimum flow velocities. Therefor it is vital to keep both flows between the optimum characterized flow rates.

Micro-bullets are conventional method of fabricate different hydrogel types. Molding process can be used for different applications such as: bacteria growth, encapsulation of cells and mimicking the tissue architecture.

5.5 Conclusion

Micro-bullet fabrication is a more convenient method for without a complexity which can provide hemispherical fabrication of PEGDA. Due to the less complexity comparing to the spheres it could be used as a fast mechanism to fabricate hydrogel structures for experiments with least resources. PEGDA microspheres have many different applications such as: drug delivery due to the microstructure and fast drug releasing capability due to the porous structure. Wide verity of applications can be addressed for both micro-bullets and microspheres due to the tissue like structure with high robustness.

CHAPTER VI

SUMMARY

This thesis demonstrates about different types of hydrogel micro-structures and their application. Applications have been focused on approaches of bio-medical conceptual mechanisms, how different hydrogels can be used according to different type of cell. As an example, Collagen and Laminin based matrigel has been applied for breast cancer cells due to their cell trapping mechanism, while PEGDA hydrogel has been used for bacteria encapsulation due to their stiffness and porous structure for nitrification applicability. Meanwhile both scenarios of cancer metastasis and bacteria encapsulation for long term analysis demonstrate the bio-compatibility of polymer based hydrogels due to the lack of contaminations. On the other hand, hydrogel microstructures were able to work with cells without harming their biological functionality and their biological behavior.

Metastasis device has been tested for different scenarios of: MDA 231, starved cells, MCF 7 cells and active cancer cells with chemo-drug. All these cells were used immediately after incubation by removing the excessive trypsin by centrifuging to keep them functional. Meanwhile, testing was done with aggressive cancer cell MDA 231 and non-metastasis cancer cell type of MCF 7. Both types resulted 20cells metastasis and zero cell metastasis while starvation MDA 231 cells resulting 8 cells to metastasis over the time. Therefore, the tested results demonstrate similar capabilities to the theoretical standards. Taking overall chip in to account it proves the miniaturize chip proven to be an advanced testing component for in-vitro analysis.

Bacteria encapsulation addresses two innovative techniques of layer by layer 3D fabrication and PEGDA hydrogel bio-compatibility with AOB/NOB bacteria cell types. Oxygen and culture media permeability is a vital requirement when it comes to the application described in the thesis, due to the oxidization and cell viability. As tested in cell viability, cells were able to stay alive and function for long term according to the application. Stiffness is another concern when it comes to bacteria encapsulation. The cells are cultured inside a glass container on a plate shaker inside a dark room. Using a more fragile structure could rupture the structure and contaminate the cells. However the PEGDA structure was able to hold their structure without any drawbacks.

Many literatures have discussed about making a single layer of hydrogel structure using a PDMS mold, although none discussed about making a multiple layer by layer structure due to many drawbacks such as alignment issue. Most of the dual encapsulations were done using flow-focusing method due to the ease of application. However, fluid method doesn't work in certain application scenario due to the oil contamination. It is necessary to use oil or a hydrocarbon type for the flow-focusing. Using a photo mask is the next method as most of the literature papers describes. Photo mask has a drawback of minimum 500um clearance area as we tested for the preliminary testing. Since the middle layer is sitting 200um apart from each island, that particular approach won't be suitable for this application. Therefore, using the layer by layer technique comes out to be the best innovative application for this particular scenario.

Formation of microstructures has been the main focus of this thesis for vital analysis mechanism. Drug delivery is another aspect of the microstructures for targeted

analysis such as chemo treatments. It will allow the scientists to do the screening in real world application development. PEGDA structures such as micro-bullet structure and microspheres are more sophisticated due to their inject ability in to the human. Encapsulation comes more vital in a real world application since the required drug dosage can be encapsulated. Drug releasing will become less complex due to the diffusive structure in the PEGDA porous membrane.

REFERENCES

[1] Gabel, C. V., Gabel, H., Pavlichin, D., Kao, A., Clark, D. A., & Samuel, A. D. (2007). Neural circuits mediate electrosensory behavior in Caenorhabditis elegans. The Journal of Neuroscience, 27(28), 7586-7596.

[2] Jemal, A., Siegel, R., Xu, J., & Ward, E. (2010). Cancer statistics, 2010. CA: A Cancer Journal for Clinicians, 60(5), 277-300.

[3] Hughes, C. S., Postovit, L. M., & Lajoie, G. A. (2010). Matrigel: a complex protein mixture required for optimal growth of cell culture. Proteomics, 10(9), 1886-1890.

[4] Jikko, A., Harris, S. E., Chen, D. I., Mendrick, D. L., & Damsky, C. H. (1999). Collagen Integrin Receptors Regulate Early Osteoblast Differentiation Induced by BMP-2. Journal of Bone and Mineral Research, 14(7), 1075-1083.

[5] Enderling, H., Alexander, N. R., Clark, E. S., Branch, K. M., Estrada, L., Crooke, C., & Weaver, A. M. (2008). Dependence of invadopodia function on collagen fiber spacing and cross-linking: computational modeling and experimental evidence. Biophysical Journal, 95(5), 2203-2218.

[6] Stordal, B., & Davey, M. (2007). Understanding cisplatin resistance using cellular models. IUBMB Life, 59(11), 696-699.

[7] Brito, D. A., Yang, Z., & Rieder, C. L. (2008). Microtubules do not promote mitotic slippage when the spindle assembly checkpoint cannot be satisfied.The Journal of Cell Biology, 182(4), 623-629.

[8] Satoh, T. H., Surmacz, T. A., Nyormoi, O., & Whitacre, C. M. (2003). Inhibition of focal adhesion kinase by antisense oligonucleotides enhances the sensitivity of breast cancer cells to camptothecins. BIOCELL-MENDOZA, 27(1), 47-56.

[9] Haidar, A., Wigglesworth, J. S., & Krausz, T. (1990). Type IV collagen in developing human lung: a comparison between normal and hypoplastic fetal lungs. Early Human Development, 21(3), 175-180.

[10] Li, Y., & Zhao, D. (2013). Basics of Molecular Biology. In Molecular Imaging, 541-601.

[11] Golbik, R., Eble, J. A., Ries, A., & Kühn, K. (2000). The spatial orientation of the essential amino acid residues arginine and aspartate within the α1β1 integrin recognition site of collagen IV has been resolved using fluorescence resonance energy transfer. Journal of Molecular Biology, 297(2), 501-509.

[12] Hain, P., Lamerdin, J., Larimer, F., Regala, W., Lao, V., Land, M., & Arp, D. (2003). Complete genome sequence of the ammonia-oxidizing bacterium and obligate chemolithoautotroph Nitrosomonas europaea. Journal of Bacteriology,185(9), 2759-2773.

[13] Guštin, S., & Marinšek-Logar, R. (2011). Effect of pH, temperature and air flow rate on the continuous ammonia stripping of the anaerobic digestion effluent.Process Safety and Environmental Protection, 89(1), 61-66.

[14] Starkenburg, S. R., Chain, P. S., Sayavedra-Soto, L. A., Hauser, L., Land, M. L., Larimer, F. W., Hickey, W. J. (2006). Genome sequence of the chemolithoautotrophic nitrite-oxidizing bacterium Nitrobacter winogradskyi Nb-255. Applied and Environmental Microbiology, 72(3), 2050-2063.

[15] Wagner, M., Rath, G., Koops, H. P., Flood, J., & Amann, R. (1996). In situ analysis of nitrifying bacteria in sewage treatment plants. Water Science and Technology, 34(1), 237-244.

[16] Nicodemus, G. D., & Bryant, S. J. (2008). Cell encapsulation in biodegradable hydrogels for tissue engineering applications. Tissue Engineering Part B: Reviews, 14(2), 149-165.

[17] Huang, G., Zhang, X., Xiao, Z., Zhang, Q., Zhou, J., Xu, F., & Lu, T. J. (2012). Cell-encapsulating microfluidic hydrogels with enhanced mechanical stability.Soft Matter, 8(41), 10687-10694.

[18] Anderson, S. B., Lin, C. C., Kuntzler, D. V., & Anseth, K. S. (2011). The performance of human mesenchymal stem cells encapsulated in cell-degradable polymer-peptide hydrogels. Biomaterials, 32(14), 3564-3574.

[19] Xia Y., Whitesides G., & Angew Chem. Int. Ed., 1998, 37, 550–575.

[20] Lorenz, H., Despont, M., Fahrni, N., Brugger, J., & Vettiger, P., & Renaud, P. (1998). High-aspect-ratio, ultrathick, negative-tone near-UV photoresist and its applications for MEMS. Sensors and Actuators A: Physical, 64(1), 33-39.

[21] Long, Z., Shen, Z., Wu, D., Qin, J., & Lin, B. (2007). Integrated multilayer microfluidic device with a nanoporous membrane interconnect for online coupling of solid-phase extraction to microchip electrophoresis. Lab Chip, 7(12), 1819-182.

[22] Jo, B. H., Van Lerberghe, L. M., Motsegood, K. M., & Beebe, D. J. (2000). Three-dimensional micro-channel fabrication in polydimethylsiloxane (PDMS) elastomer. Microelectromechanical Systems, Journal of, 9(1), 76-81.

[23] Nuttelman, C. R., Tripodi, M. C., & Anseth, K. S. (2005). Synthetic hydrogel niches that promote hMSC viability. Matrix Biology, 24(3), 208-218.

[24] Alexandridis, P. (1997). Poly (ethylene oxide)/poly (propylene oxide) block copolymer surfactants. Current Opinion In Colloid & Interface Science, 2(5), 478-489.

[25] Liu, V. A., & Bhatia, S. N. (2002). Three-dimensional photopatterning of hydrogels containing living cells. Biomedical Microdevices, 4(4), 257-266.

[26] Han, J. H., Heinze, B. C., & Yoon, J. Y. (2008). Single cell level detection of Escherichia coli in microfluidic device. Biosensors and Bioelectronics,23(8), 1303-1306.

[27] Park, G. E., Oh, H. N., & Ahn, S. (2009). Improvement of the ammonia analysis by the phenate method in water and wastewater. Bull Korean Chem Soc, 30, 2032-2038.

[28] Dytczak, M. A., Londry, K. L., & Oleszkiewicz, J. A. (2008). Activated sludge operational regime has significant impact on the type of nitrifying community and its nitrification rates. Water Research, 42(8), 2320-2328.

[29] Chan, C., Chang, S., & Naguib, H. E. (2010, January). A Parametric Study and Characterization of Porous, Non-Permeable, and Conductive PEGDA-HEMA

Hydrogels. In ASME 2010 Conference on Smart Materials, Adaptive Structures and Intelligent Systems, American Society of Mechanical Engineers, 89-96.

[30] Yan, J., Sun, Y., Zhu, H., Marcu, L., & Revzin, A. (2009). Enzyme-containing hydrogel micropatterns serving a dual purpose of cell sequestration and metabolite detection. Biosensors and Bioelectronics, 24(8), 2604-2610.

[31] De Clippeleir, H., Courtens, E., Mosquera, M., Vlaeminck, S. E., Smets, B. F., Boon, N., & Verstraete, W. (2012). Efficient total nitrogen removal in an ammonia gas biofilter through high-rate OLAND. Environmental Science & Technology, 46(16), 8826-8833.

[32] Tuck, S. (2014). The control of cell growth and body size in Caenorhabditis elegans. Experimental Cell Research, 321(1), 71-76.

[33] Cassada, R. C., & Russell, R. L. (1975). The dauerlarva, a post-embryonic developmental variant of the nematode Caenorhabditis elegans. Developmental Biology, 46(2), 326-342.

[34] Brenner, S. (1974). The genetics of Caenorhabditis elegans. Genetics, 77(1), 71-94.

[35] Cascella, R., Evangelisti, E., Zampagni, M., Becatti, M., D'Adamio, G., Goti, A., & Cecchi, C. (2014). S-linolenoyl-glutathione intake extends lifespan and stress resistance via SIR-2.1 upregulation in Caenorhabditis elegans. Free Radical Biology & Medicine, Volume 73, August 2014, Pages 127-135

[36] Byerly, L., Cassada, R. C., & Russell, R. L. (1976). The life cycle of the nematode Caenorhabditis elegans:I.Wild-type growth and reproduction. Developmental Biology, 51(1), 23-33.

[37] Herrmann, I. K., Schlegel, A., Graf, R., Schumacher, C. M., Senn, N., Hasler, M., & Beck-Schimmer, B. (2013). Nanomagnet-based removal of lead and digoxin from living rats. Nanoscale, 5(18), 8718-8723.

[38] Mata, A., Fleischman, A. J., & Roy, S. (2006). Fabrication of multi-layer SU-8 microstructures. Journal of Micromechanics and Microengineering, 16(2), 276.

[39] Lim, S. F., Riehn, R., Ryu, W. S., Khanarian, N., Tung, C. K., Tank, D., & Austin, R. H. (2006). In vivo and scanning electron microscopy imaging of upconverting nanophosphors in Caenorhabditis elegans. Nano Letters, 6(2), 169-174.

[40] Peng, C., Zhang, Y., Tong, W., & Gao, C. (2011). Influence of folate conjugation on the cellular uptake degree of poly (allylamine hydrochloride) microcapsules. Journal of Applied Polymer Science, 121(6), 3710-3716.

[41] García-Alonso, J., Fakhrullin, R. F., & Paunov, V. N. (2010). Rapid and direct magnetization of GFP-reporter yeast for micro-screening systems. Biosensors and Bioelectronics, 25(7), 1816-1819.

[42] Wang, L., Yang, Z., Zhang, Y., & Wang, L. (2009). Bifunctional nanoparticles with magnetization and luminescence. The Journal of Physical Chemistry C,113(10), 3955-3959.

[43] Däwlätşina, G. I., Minullina, R. T., & Fakhrullin, R. F. (2013). Microworms swallow the nanobait: the use of nanocoated microbial cells for the direct delivery of nanoparticles into Caenorhabditis elegans. Nanoscale, 5(23), 11761-11769.

[44] Stiernagle, T. (1999). Maintenance of C. elegans. C. Elegans: A Practical Approach, 51-67.

[45] Zheng, Y., Brockie, P. J., Mellem, J. E., Madsen, D. M., & Maricq, A. V. (1999). Neuronal Control of Locomotion in C. elegans Is Modified by a Dominant Mutation in the GLR-1 Ionotropic Glutamate Receptor. Neuron, 24(2), 347-361.

[46] Sznitman, J., Shen, X., Sznitman, R., & Arratia, P. E. (2010). Propulsive force measurements and flow behavior of undulatory swimmers at low Reynolds number. Physics of Fluids (1994-Present), 22(12), 121901.

[47] Leiers, B., Kampkötter, A., Grevelding, C. G., Link, C. D., Johnson, T. E., & Henkle-Dührsen, K. (2003). A stress-responsive glutathione S-transferase confers resistance to oxidative stress in Caenorhabditis elegans. Free Radical Biology and Medicine, 34(11), 1405-1415.535.

[48] Rezai, P., Salam, S., Selvaganapathy, P. R., & Gupta, B. P. (2012). Electrical sorting of Caenorhabditis elegans. Lab On a Chip, 12(10), 1831-1840.

[49] Nemir, S., Hayenga, H. N., & West, J. L. (2010). PEGDA hydrogels with patterned elasticity: novel tools for the study of cell response to substrate rigidity. Biotechnology and Bioengineering, 105(3), 636-644..

[50] Durst, C. A., Cuchiara, M. P., Mansfield, E. G., West, J. L., & Grande-Allen, K. J. (2011). Flexural characterization of cell encapsulated PEGDA hydrogels with applications for tissue engineered heart valves. Acta Biomaterialia, 7(6), 2467-2476..

[51] Wu, J., Zhao, Q., Sun, J., & Zhou, Q. (2012). Preparation of poly (ethylene glycol) aligned porous cryogels using a unidirectional freezing technique. Soft Matter, 8(13), 3620-3626.

[52] Hong, S., Hsu, H. J., Kaunas, R., & Kameoka, J. (2012). Collagen microsphere production on a chip. Lab On a Chip, 12(18), 3277-3280.

[53] Yang, C. H., Huang, K. S., Lin, P. W., & Lin, Y. C. (2007). Using a cross-flow microfluidic chip and external crosslinking reaction for monodisperse TPP-chitosan microparticles. Sensors and Actuators B: Chemical, 124(2), 510-516.

[54] Nie, Z., Li, W., Seo, M., Xu, S., & Kumacheva, E. (2006). Janus and ternary particles generated by microfluidic synthesis: design, synthesis, and self-assembly. Journal of the American Chemical Society, 128(29), 9408-9412.

APPENDIX A

PEGDA synthesis process

Day 0

1) Glassware should be dried overnight at 100^{o}C
2) Measure 24g of 10000MW PEG power in to a beaker
3) Pour the powder in to the beaker and cover and seal with a kim wipe, leave inside vacuumed for overnight

Day1

4) Combine 24g of PEG 10000MW with dry DCM (Di-Chloro Methene) 120ml inside a sealed round bottom flask
5) Stir overnight with a magnetic stir bar for 1 day

Day 2

6) Purge the vessel with Nitrogen for 5 minutes, 2 needles used one for the Nitrogen purging, while other needle for the exhaust
7) Stop the Nitrogen Valve and take out the exhaust needle
8) Add 0.67ml of 0.0008mol Triethylamine via a glass syringe
9) Add 0.78ml of Acryloyl Chloride 0.016mol via a glass syringe
10) Remove the Nitrogen inlet needle and stir with the magnetic stir bar overnight

Day 3

11) Transfer liquid on to a 250ml separatory funnel
12) Wash the round bottom flask with 20ml of DCM and add the liquid to the funnel

13) Add 9.6ml of K_2CO_3 in to the funnel
14) Shake and remove the CO_2 via the valve, repeat this several times until all the CO_2 pass through the valve
15) Color will change to milky white
16) Cover the top with a parafilm and leave overnight straight hanging from upright with the valve towards the bottom

Day 4

17) It is visible the two layers are separate
18) Remove the film and add 10ml of DCM and 10ml of DI water and shake vigorously
19) Leave 10mins until two layers are separate
20) Leave a 500ml dry beaker under the valve and collect the bottom part of the layer carefully
21) Add $MgSO_4$ 10g and stir with a magnetic stir bar for 15mins in order to remove the water
22) Pour the solution via #1 Filter paper under the vacuum in to a vacuum flask
23) Add 15ml of dry DCM on to the filter paper
24) Add 500ml of diethyl either on to the filter paper
25) Place a 2L beaker on the magnetic plate and add 500ml of diethyl either
26) Pour the solution from vacuum flask on to the 2L beaker while stirring with the magnetic bar
27) Stir for 15mins

28) Place a #2 filter paper in to the flask funnel

29) Pour the solution under the vacuum

30) Collect the remaining PEGDA from the #2 filter paper

31) Cover with a foil wrap and keep in a dry place

Day 5

32) Crush the PEGDA solids with a mortar and presell

33) Keep the powder inside a 250ml beaker and seal with a kim wipe

34) Vacuum dry for overnight, while releasing the vacuum after 1hr, 2hr, 3hr intervals.

35) Then release the vacuum after every 3 hr during 18hr time period

36) Pour the powder in to a glass bottle and close the cap

37) Seal the cap with a para film and store in a dry place